Coordination Chemistry Reviews 253 (2009) 1947–1965

Contents lists available at ScienceDirect

Coordination Chemistry Reviews

journal homepage: www.elsevier.com/locate/ccr

Review

Developments in tellurium containing macrocycles

Arunashree Panda*

Chemistry Group, Birla Institute of Technology and Science, Pilani-Goa Campus, Goa 403 726, India

Contents

ARTICLE INFO

Article history:
Received 7 October 2008
Accepted 27 March 2009
Available online 5 April 2009

Keywords:
Tellurium
Macrocycles
Cryptand
Porphyrin
Schiff base

ABSTRACT

The chemistry of tellurium containing macrocycles starting from the report of the first macrocyclic organotellurium(IV) chelates in 1982 is reviewed.

1. Introduction

Tellurium is a silvery white and semi-metallic rare element. Organotellurium ligands find uses in organic chemistry, precursors for metal-organic chemical vapor deposition (MOCVD) of semiconducting materials, ligand chemistry, biochemistry, etc. Over recent years, considerable effort has been directed towards the design and synthesis of telluroether macrocyclic ligands. However, while several macrocyclic selenoethers are now known, telluroether crowns are still rare. The large size of tellurium atom and the electronegativity difference of Te and C atoms make Te–C bond more polarizable. The high reactivity of the Te–C bond compared to S–C and Se–C bonds along with the toxicity of the organotellurium compounds has held back research in this area. Polyselenoether macrocycles have been shown to exhibit rich coordination chemistry for a wide range of d- and p-block elements [1–6]. The introduction of tellurium atoms into a macrocycle adds an additional probe, i.e. ^{125}Te NMR which would give invaluable structural information about the macrocyclic ligands and complexes in solution and this has enhanced the interest in telluromacrocycles. ^{125}Te is a spin 1/2 nucleus with a receptivity of *ca.* 12.5 times that of ^{13}C nucleus, a natural abundance of 7% and a very large chemical shift range. Moreover, the lower electronegativity of Te combined with its greater s electron properties over S and Se [7] should yield lig-

Abbreviations: S2TPP, tetraphenyl-21,23-dithiaporphyrin; S,TeTPP, tetraphenyl-21-tellura-23-thiaporphyrin; Te2TPP, 5,10,15,20-tetraphenyl-21,23-ditelluraporphyrin; 8Te2, 1,5-ditelluracyclooctane; 9S2Te, 1,4-dithia-7-telluracyclododecane; 11S2Te, 1,4-dithia-8-telluracycloundecan; 12S2Te, 1,5-dithia-9-telluracyclododecane; 18O4Te2, 1,10-ditellura-4,7,13,16-tetraoxacyclooctadecane; 9O2Te, 1-tellura-4,7-dioxacyclononane; Dic-Te, 4′-(2-pyridylmethyleneamino)-benzo-10-tellura-15-crown-5; 12Te3, 1,5,9-tritelluradodecane.

* Tel.: +91 832 2580389; fax: +91 832 2557033.
E-mail address: panda_arunashree@yahoo.com.

0010-8545/$ – see front matter © 2009 Elsevier B.V. All rights reserved.
doi:10.1016/j.ccr.2009.03.025

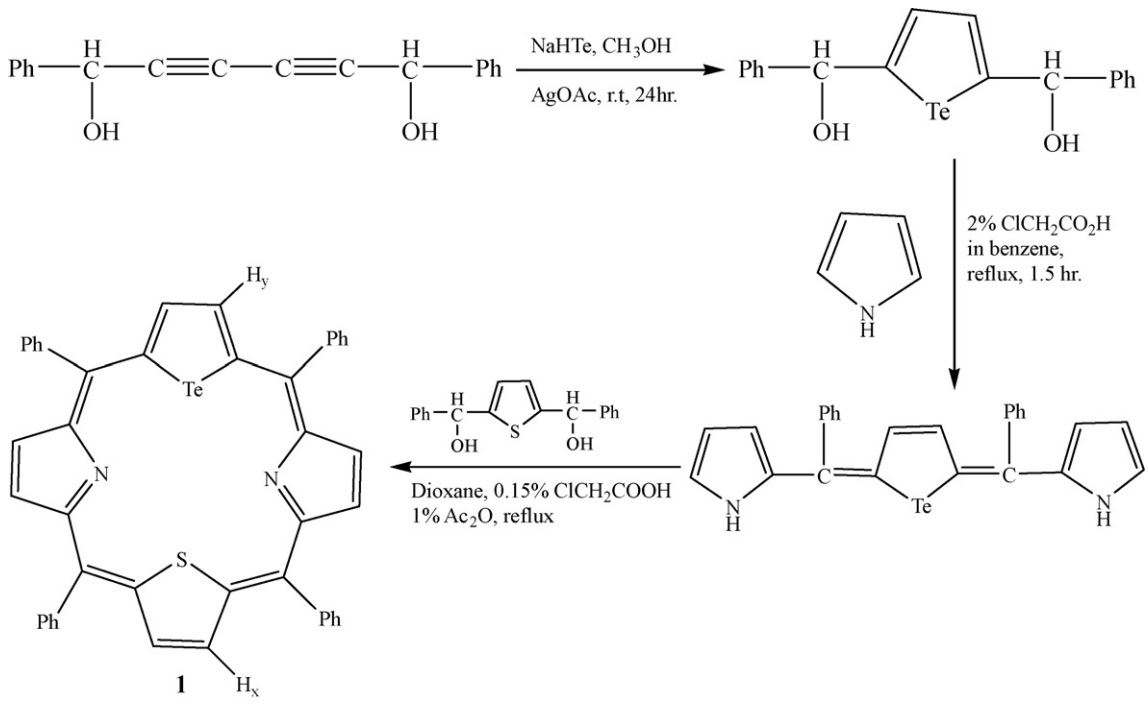

Scheme 1.

ands capable of rich coordination chemistry. Of additional interest is the possibility to obtain macrocycles that contain mixed-donor functionalities. Macrocycles of this type, especially those containing both hard and soft donor atoms, are of immense interest since they can potentially bind two metals of differing character and oxidation state within the same cavity. Some smaller fragments of this topic has been included in the review articles on somewhat broader topics of tellurium ligands by Singh and Sharma [8], Levason and Reid [9], Levason et al. [3], Levason and Reid [4]. This systematic presentation of the overall developments of tellurium containing macrocycles is intended to promote interest among researchers in this field.

2. Telluraporphyrins

There are few reports on core-modified porphyrins where the NH fragment is replaced by a tellurium atom in the 21-position and is opposite to NH or S atom at the 23-position [10–19]. The larger van der Waals radii of the heteroatoms in the core modified porphyrins enforce 21-heteroatom–23-heteroatom contact. Ulman and coworkers [10] reported the first core-modified telluraporphyrin i.e. tetraphenyl-21-tellura-23-thiaporphyrin (S,TeTPP, **1**) (Scheme 1). An abnormally short Te···S distance (2.65 Å) was found from the X-ray structure of **1**.

X-ray structure analysis on heterosubstituted tetraphenylporphyrins, where two NH groups in the core are replaced by S, Se and Te (Fig. 1), shows abnormally short distances between the heteroatoms X and Y (X, Y = S, Se, Te) indicating chemical bonding interactions between the heteroatoms which is further supported by high resolution NMR study [11]. This interaction, which increases in the order S, Se, Te, changes the inner and outer aromatic pathway of the porphyrin and influences the chemical shifts of the hydrogen atoms H_x and H_y at the periphery of the molecule [11]. The latter can be explained from the Kekulé structures for porphyrin. Fig. 1 shows the possible Kekulé structures for the heterosubstituted porphyrins. The 16-, 18- and 20-membered structures correspond to the inner, outer and extended outer aromatic pathway respectively. The statistical weight of the outer aromatic pathway (18-membered) increases with the increase in X···Y interaction leading to lesser electron density available on X and Y for the inner aromatic pathway. This results in the downfield shifts of H_x and H_y (since these are closer to the outer aromatic pathway) compared to the symmet-

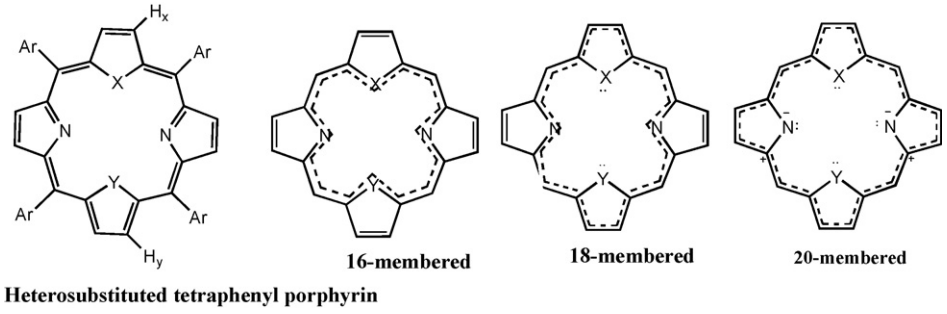

Fig. 1. Heterosubstituted tetralphenylporphyrin and relevant Kekulé structures for the porphyrin molecule.

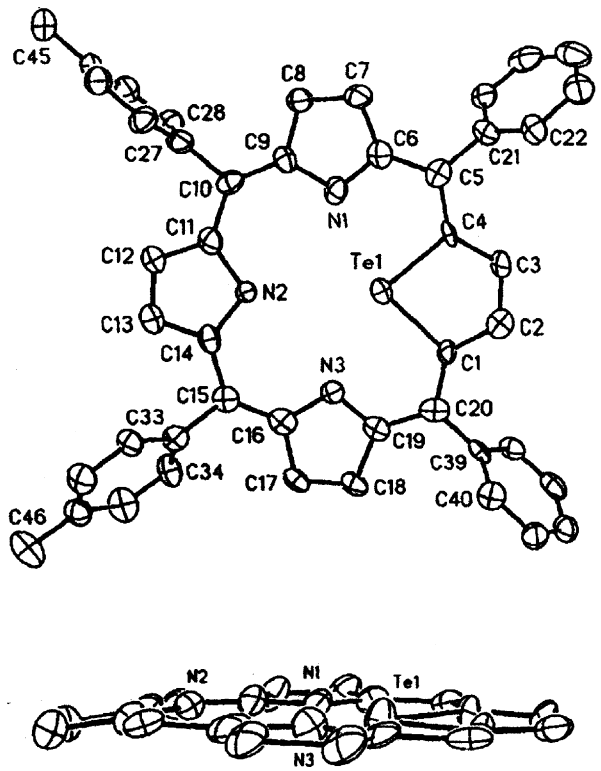

Fig. 2. Two views of the crystal structure of the 21-telluraporphyrin **2** (Ar = *p*-$CH_3C_6H_4$, Ar′ = C_6H_5). The lower drawing emphasizes the deviation from planarity. Taken from Ref. [12] with permission from the corresponding authors. Copyright Wiley-VCH Verlag GmbH and Co. KGaA. Reproduced with permission.

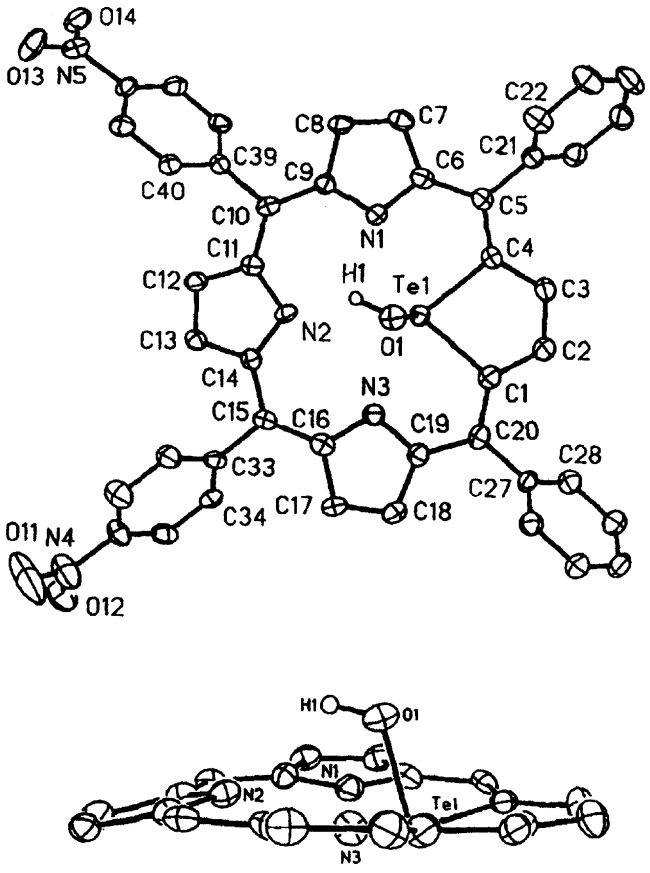

Fig. 3. Two views of the crystal structure of **4** (Ar = *p*-$O_2NC_6H_4$ and Ar = C_6H_5). Taken from Ref. [12] with permission from the corresponding authors. Copyright Wiley-VCH Verlag GmbH and Co. KGaA. Reproduced with permission.

rically substituted porphyrins in NMR spectrum. These downfield shifts are not due to changing electronegativity of the heteroatoms as found for free heterocycles because breaking the bonding X···Y interaction within the core, either by protonation or complexation, results in upfield shifts of H_x and H_y. These upfield shifts are due to the contributions of full electron density of heteroatoms to the inner aromaticity and thus decreasing the relative probability of outer aromaticity. In **1**, charge transfer occurs from Te to S owing to the Te···S interaction. Therefore, there is more inner aromaticity through S in S,TeTPP than in the symmetrical S2TPP and hence an upfield shift of thiophene-H (H_x) of S,TeTPP is observed compared to H_x of S2TPP. Similarly, less electron density is available on Te for the inner aromatic pathway resulting in a downfield shift of H_y.

The 21-telluraporphyrins **2** have been synthesized according to Scheme 2 [12]. The structure of **2** (Ar = *p*-$CH_3C_6H_4$, Ar′ = C_6H_5) shows a longer nonbonded N1···N3 distance relative to that in a normal porphyrin due to the larger size of the tellurium atom and thus the macrocycle of **2** is distorted (Fig. 2). Despite the short Te···N(2) distance, this porphyrin macrocycle with large core heteroatom is almost planar. This suggests the involvement of the tellurophene ring in aromatic delocalization unlike the selenaporphyrin analog. In contrast to its thia and selena counterparts, 21-telluraporphyrins **2** are air sensitive and can be converted into the 21-oxaporphyrins **3** when treated with *m*-chloroperoxybenzoic acid. This reaction proceeds *via* the formation of novel tellurium hydroxyl compound **4** (Scheme 2). The oxygen at the tellurium deprotonates the pyrrole ring forming a new compound **4** with a hydroxyl group at tellurium atom. The facile oxidation of the tellurium atom in the tellurophene unit in **2** and its conversion into a furan upon treatment with a peroxy acid are unusual in tellurophene chemistry. The reactions of the macrocycle **2** demonstrated the remarkable ability of the porphyrin environment to alter the fundamental reactivity of the tellurophene portion. The X-ray crystal structure of **4** (Ar = *p*-$O_2NC_6H_4$ and Ar = C_6H_5) shows that the telluroxide O is protonated by the pyrrole NH *trans* to the tellurophene ring and thus produces a zwitterions with a hydroxy group attached to the tellurium atom (Fig. 3). The most interesting structural feature of **4** is that the Te–O bond passes through the porphyrin plane. The hydroxy group attached to the tellurium atom forms a weak hydrogen bond with the deprotonated nitrogen atom of the *trans* pyrrol ring which is tipped out of plane toward the hydroxyl group.

The fragile nature of the C–Te–C fragment makes **2** (Ar = *p*-$CH_3C_6H_4$ and Ar′ = C_6H_5) [12] a good candidate to synthesize a novel molecule, aza-deficient porphyrin 5,10,15,20-tetraaryl-21-vacataporphyrin, by subtracting the tellurium atom from **2** [13].

Organotellurides act as catalyst for the activation of H_2O_2 [14]. Mechanistic studies have shown that the initial oxidation of organotelluride with H_2O_2 leads to diorganodihydroxy tellurane, ($R_2Te(OH)_2$), a Te(IV) compound. This is followed by ligand exchange which in turns undergoes reductive elimination to regenerate the organotelluride. In the case of tellurium containing 21- and 21,23-core-modified porphyrins, the heteroatom at 23-position stabilizes the Te(IV) intermediates by donating a lone pair of electrons.

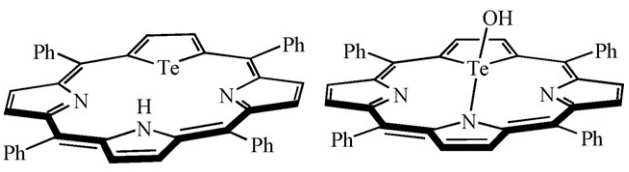

5 **6**

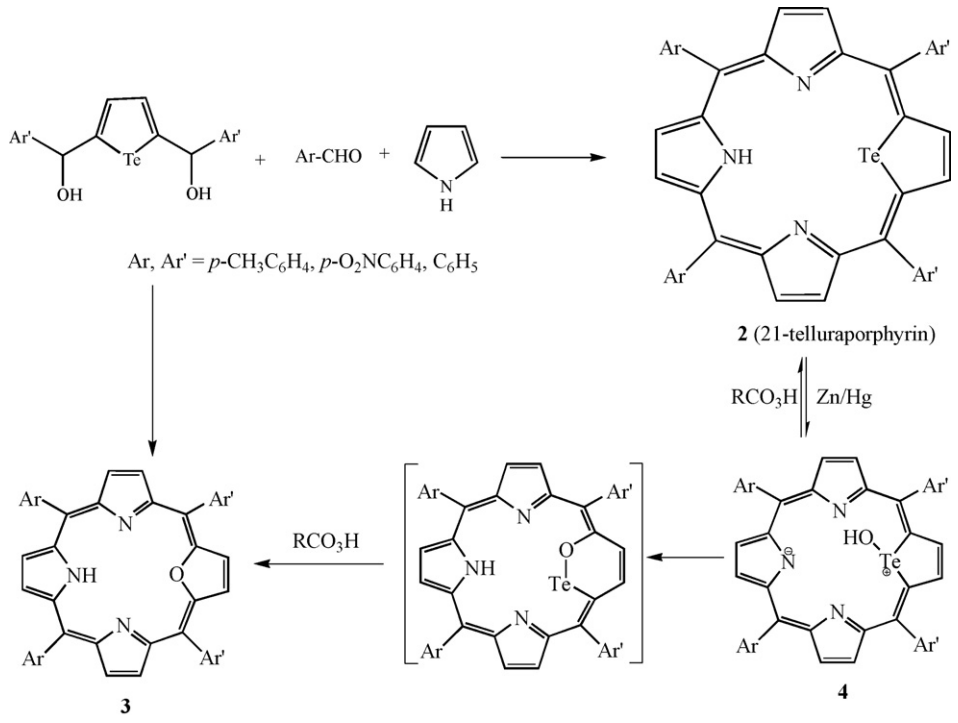

Scheme 2.

The reaction of benzaldehyde, pyrrol and a 2,5-bis(phenylhydroxymethyl)tellurophene gives 21-telluraporphyrin (**5**). However, in the presence of light the same reaction gives the oxidized telluraporphyrin (**6**), a product from the chemical oxidation of **5** with air or H_2O_2 [15]. This facile air oxidation of **5** is supported by cyclic voltammetry and spectroscopic studies. The cyclic voltammetry studies show the electrochemical oxidation of 21-telluraporphyrins (**5** and **1**) at a more negative potential than for the lighter chalcogen analogues. The easier oxidation is attributed to the larger size of the tellurium atom which leads to a distortion in the planarity of the 21-telluraporphyrin due to 21-tellurium-23-heteroatom interactions in solution. The oxidation of 21-telluraporphyrin (**5**) with H_2O_2 proceeds with a second order rate constant. All these observations suggest the usefulness of 21-telluraporphyrins as catalysts for the activation of H_2O_2. The 23-heteroatom facilitates oxidation and acts as a back donor to block the approach from one side while forcing oxidizable substrates to approach the tellurium center only from the other direction. Compounds **1** and **5** also act as catalysts for bromination reactions with H_2O_2 and NaBr; compound **1** is much less efficient as a catalyst than compound **5** [16]. Surprisingly, 21-thia/selenaporphyrins and 21,23-dithia/diselenaporphyrins do not display any catalytic activity in the bromination of 4-pentenoic acid with H_2O_2 and NaBr.

Detty and coworkers [17] have also reported a telluraporphyrin of the type 5,10-diphenyl-15,20-di(4-methoxyphenyl)-21-telluraporphyrin (**7**) and the novel Te(IV) derivative, 21,21-dihalo-21-telluraporphyrin (**8**). The amine hydrogen atom is delocalized among the pyrrole rings and hence three tautomeric forms are present for **7** (Scheme 3). The crystal structure of **7** (Fig. 4) is of a tautomer with the pyrrole N–H *cis* to the tellurophene which is not observed in other 21-telluraporphyrin [12]. The core of the porphyrin is basically planar. The oxidation of 21-telluraporphyrin (**7**) to its corresponding telluroxide followed by the ligand exchange with chloride gives the novel 21,21-dichloro-21-telluraporphyrin (**8**). The structure shows the tellurium to be in a distorted trigonal bipyramidal geometry, which is typical of diorganotellurium(IV) dihalides, with the Te–Cl bonds in *trans*-axial positions (Fig. 5). The molecule is distorted from the ideal trigonal bipyramidal geometry because of the greater stereochemical influence of the non-bonding pair of electrons that can be seen from the Cl–Te–Cl and C–Te–C bond angles (Table 1). The direction of bend of the axial angles is consistent with the prediction of the VSEPR model [20] and is similar to that observed in all other Te(IV) macrocycles (*vide infra*). Both

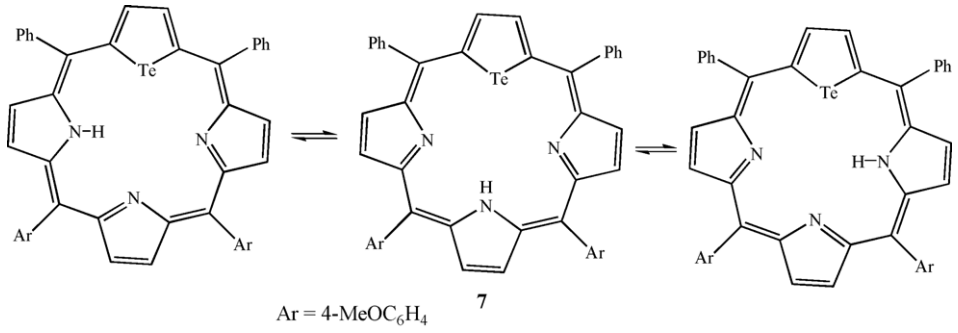

Scheme 3.

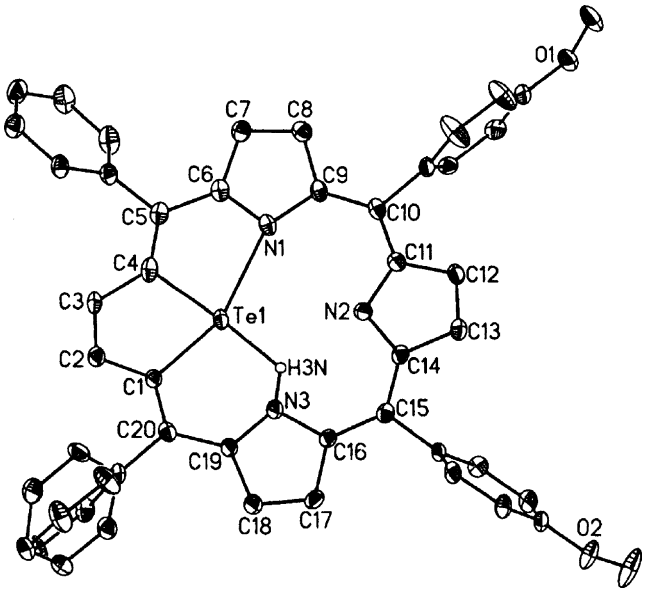

Fig. 4. Molecular structure of **7**. Reprinted with permission from [17]. Copyright (2004) American Chemical Society.

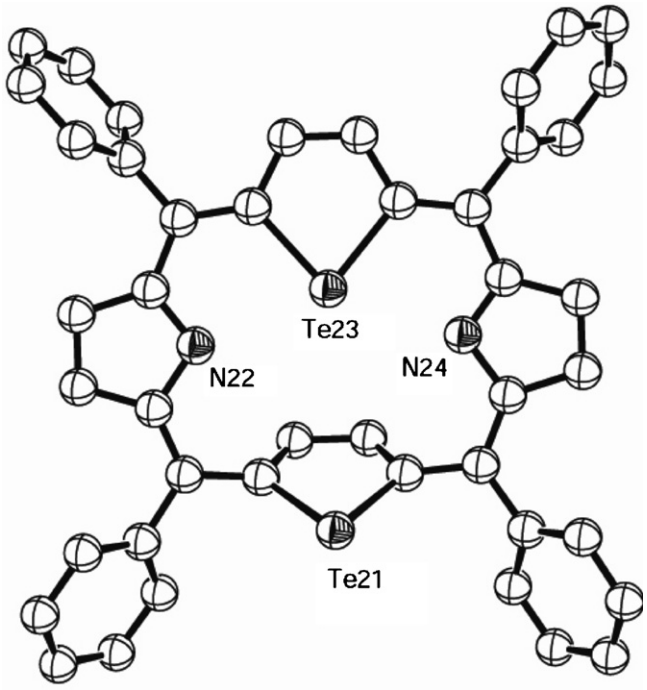

Fig. 6. The crystal structure of **Te2TPP**. Taken from Ref. [18] with permission from the corresponding authors. Copyright Wiley-VCH Verlag GmbH and Co. KGaA. Reproduced with permission.

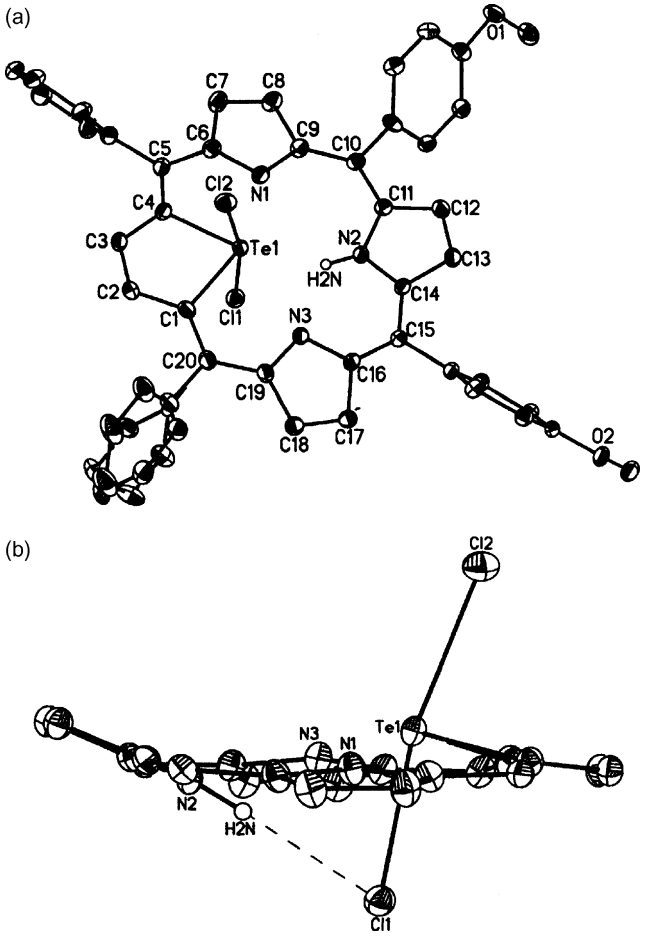

Fig. 5. Molecular structure of **8** (a) top and (b) side view. Reprinted with permission from [17]. Copyright (2004) American Chemical Society.

Te and N (of the *trans* pyrrole) are tipped out of the plane and hence there is a nonplanar porphyrin core similar to **4** [12], but in contrast to the planar core of **7** and **2**. Since the Te1 and N2 are turned out of the plane in **8**, the non-bonded Te1···N2 distance is longer than the corresponding distance in **7**. The Te atom does not take part in porphyrin aromaticity as the tellurophene ring of **8** is distorted from planarity.

5,10,15,20-Tetraphenyl-21,23-ditelluraporphyrin (**Te2TPP**) is the first heteroanalogue of [18] porphyrin-(1.1.1.1) [18]. One of the tellurophene moieties (Te23) of **Te2TPP** is coplanar with two adjacent pyrrole rings while the second tellurophene is flipped and the Te21 atom is directed away from the centre of the macrocycle (Fig. 6) unlike the oxa [21], thia [22] and selena [23] diheteroporphyrin where all heteroatoms directed towards the centre of the macrocycle. The different behavior of ditelluroporphyrin is a consequence of the large size of the tellurium atom and also due to the different geometry and electronic structure of the tellurophene ring. The inverted ring is not coplanar with the rest of the macrocycle in **Te2TPP** but still is moderately aromatic. The preferred 18-π electron conjugation pathway in 21,23-ditelluraporphyrin is identical with that observed in the monoheteroporphyrins. The two tellurophene rings undergoes rapid inversion in solution *via* the uninverted one.

In summary, the tellurium-containing 21- and 21,23-core-modified porphyrins represent an interesting class of molecules. The porphyrin ring has preorganised the heteroatom to interact with the 21-tellurium atom. The bonding interactions between the heteroatoms within the porphyrin core are crucial for the stability of the molecule [10]. For example, protonation of the nitrogen atoms and complexation decrease the stability of the molecule by breaking the inner core interaction [11]. Basically, the large size of the tellurium atom fills the core and prevents endocyclic coordination of metals. 21-Telluraporphyrins acts as catalysts for bromination reactions with H_2O_2 and NaBr. An unusual alteration of the reactivity of tellurophene within a core modified telluraporphyrin environment is observed. For example (1)

Table 1
Selected bond lengths and angles for different macrocycles.

Compound no.	Bond	Length (Å)	Bond	Angle (°)
8	Te1–Cl1	2.49 (2.36)[a]	Cl1–Te1–Cl2	165.65
	Te1–Cl2	2.58	C–Te–Cl	85.39(8)–85.62(9)
	Te1···N2	3.293 (3.61)[a]	C(4)–Te–C(1)	81.8(1)
12	Te(1)–Cl(1)	2.50(1)	Cl–Te–Cl	178.2–173
	Te(1)–Cl(2)	2.49(1)	C–Te–Cl	86–92
	Te···Cl	3.35(1)–3.81(1) (3.95)[a]	C–Te–C	96–107
38	Te–O	2.133(4)–2.166(4) (2.15)[a]	O–Te–O	161.8(2)–168.3(2)
			C–Te–C	96.2(2)–100.3(2)
39	Te–O	1.99(2)–2.29(2)	O–Te–O	166.1(8)–168.7(7)
	Te···O	2.95–3.20 (3.6)[a]	C–Te–C	96(1)–101(1)
40	Te–O	2.089(8)–2.116(8)	O1–Te2–O2	167.8(3)
			C–Te–C	97.5(5)
41	Te–O	2.144(3)–2.167(3)	O–Te–O	162.80(10)–166.09(9)
			C–Te–C	99.36(15)–102.28(14)
			C–Te–O	79.67(12)–84.72(13)
42	Te–O	2.123(2)–2.129(2)	O2–Te–O1	161.62(9)
			C–Te–C	94.99(13)
			C–Te–O	81.77(12)–85.68(12)
12S2TeI2	I–Te	2.8990(9)–2.9179(9)	I(1)–Te(1)–I(2)	176.77(3)
			I–Te–C	86.3(3)–96.0(3)
			C(1)–Te(1)–C(9)	93.3(4)
11S2Te			C(1)–Te(1)–C(8)	95.5(2)
			C(3)–S(1)–C(4)	103.4(3)
			C(5)–S(2)–C(6)	100.1(3)
12S2Te			C(1)–Te(1)–C(9)	94.2(2)
			C(3)–S(1)–C(4)	101.3(2)
			C(6)–S(2)–C(7)	100.4(3)

[a] The number inside the parenthesis indicates the sum of the covalent/van der Waals radii of the corresponding atoms.

the conversion of 21-telluraporphyrin to 21-oxaporphyrins with *m*-chloroperoxybenzoic acid, (2) the formation of 21,21-dichloro-21-telluraporphyrin with HCl, and (3) the synthesis of aza-deficient porphyrin 5,10,15,20-tetraaryl-21-vacataporphyrin by subtraction of a tellurium atom from 5,10,15,20-tetraaryl-21-telluraporphyrin.

3. Homoleptic macrocyclic polytelluroethers

Furukawa and coworkers have reported a new eight-membered ring tellurium compound, 1,5-ditelluracyclooctane (**8Te2**) (Scheme 4) [24]. The novel ditelluride dication **10**, generated by two-electron oxidation of the bis-telluride **8Te2** with a one-electron-oxidizing agent, behaves as an oxidizing agent.

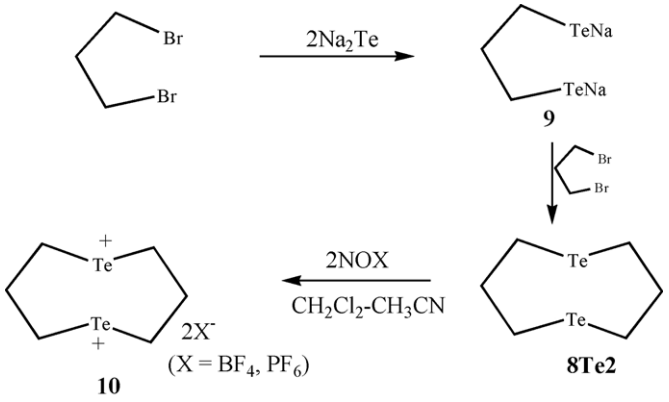

Scheme 4.

A new type of chlorine adduct of a 12-membered ring telluro-macrocycle consisting of three hypervalent tellurium(IV) moiety (**12**) is reported by the same group in 1996 from the pyrolysis of 8-membered ring compound **11** (Scheme 5) [25]. Compound **12** forms polymeric networks in the solid state by intermolecular chlorine bridges. Like most diorganotellurium(IV) dihalides, the electron pair geometry of Te(IV) atom resembles a distorted trigonal bipyramid (TBP) (Fig. 7) in which the more electronegative chlorine atoms are situated at the usual axial positions and the two alkyl carbon atoms and a lone pair occupy the three corners of the trigonal plane. The lone pair electrons appears to have no significant distorting effect upon the Cl–Te–Cl and C–Te–Cl angles but the larger vol-

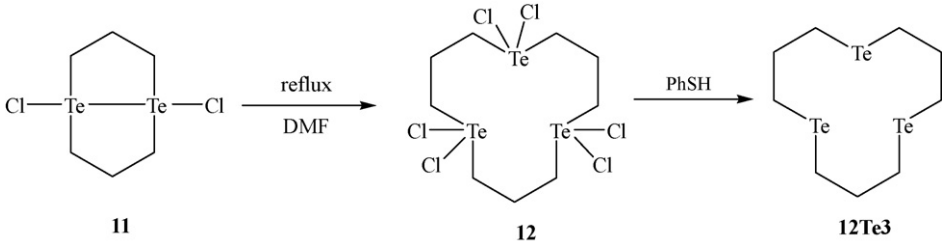

Scheme 5.

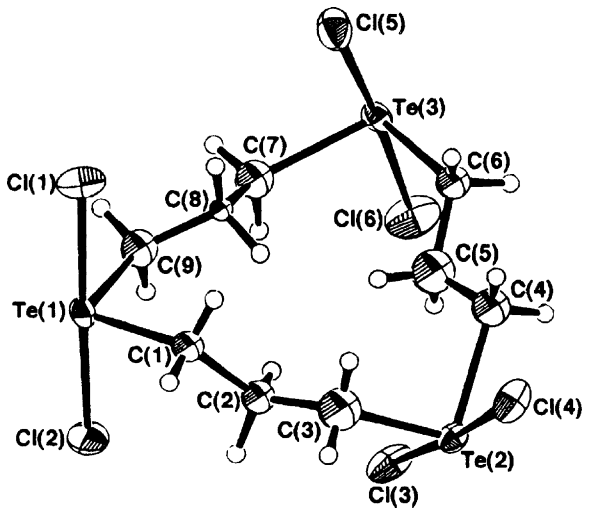

Fig. 7. ORTEP plot for the structure of **12**. Reprinted with permission from [25]. Copyright (1996) American Chemical Society.

ume of lone pairs has pushed the C–Te–C angles closer together. Though there are a number of intermolecular contacts between tellurium and chlorine atoms, which is most common among Te(IV) compounds with halogen containing ligands, there is no interaction among the intramolecular tellurium atoms. The presence of intermolecular interactions gives tellurium(IV) a coordination number higher than that expected from the compound's stoichiometry. The longer Te–Cl bond lengths (Table 1) show reduced stereochemical activity of the lone pairs. The tris(tellurane) **12** also acts as an oxidant.

4. Metallomacrocycles

The first example of a structurally characterized macrocyclic chelate involving a tellurium ligand was reported by McWhinnie and coworkers [26]. The reaction of $HgCl_2$ and 1,6-bis-2-butyl tellurophenyl-2,5-diazahexa-1,5-diene gives the 13-membered chelate ring **13**. In the complex **13**, mercury(II) is bonded to two chlorine and two tellurium atoms and the coordination geometry at mercury is tetrahedral (Fig. 8). Tellurium(II) acts simultaneously as Lewis acid and Lewis base due to the presence of both Hg–Te and

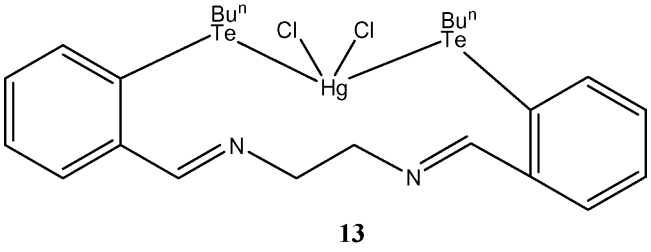

13

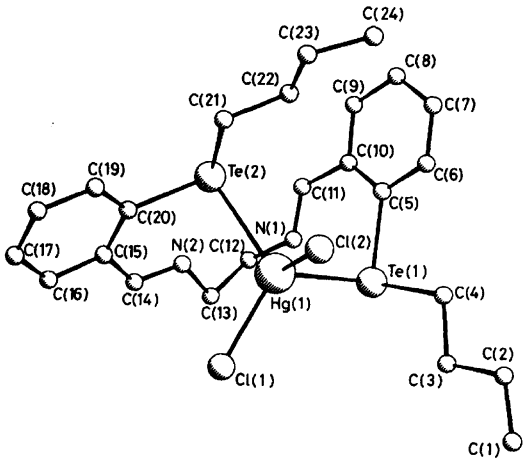

Fig. 8. The structure of the mercury complex **13**. Taken from Ref. [26]. Reproduced by permission of The Royal Society of Chemistry.

Te···N interactions. In the present structure, tellurium coordinates only to mercury despite the existence of a possible Te–N coordination to give a six-membered chelate ring and hence shows the strong preference for 'soft' acids by tellurium ligands. The decreased dentacity of the ligand is due to the engagement of the nitrogen lone pair in the formation of intramolecular Te···N bond.

The polymeric silver(I) complex of $MeTe(CH_2)_3TeMe$ consists of 24-membered $Ag_4(MeTe(CH_2)_3TeMe)_4$ metallomacrocycles in which each Ag(I) atom is coordinated by four tellurium atoms of four bridging $MeTe(CH_2)_3TeMe$ in a distorted tetrahedral manner (Fig. 9) [27]. The non-interacting $[BF_4]_n$ anions are situated between the cationic layers of $[Ag(MeTe(CH_2)_3TeMe]_n^{n+}$. Two tel-

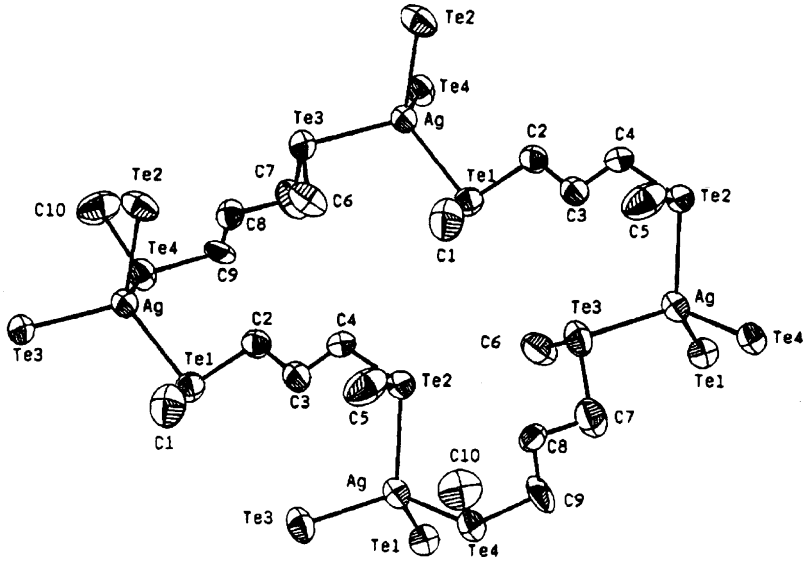

Fig. 9. ORTEP drawing of part of polymeric $[Ag(MeTe(CH_2)_3TeMe)_2]_n$ cation. Reprinted with permission from [27]. Copyright (1995) American Chemical Society.

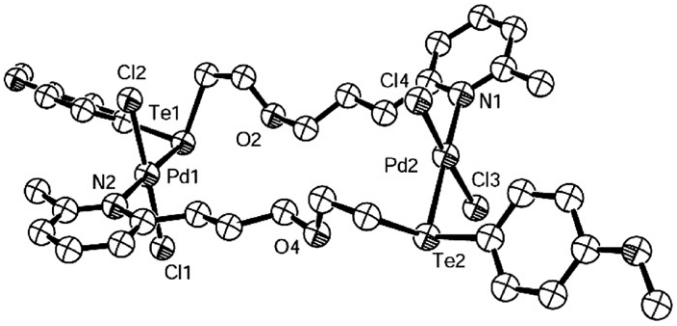

Fig. 10. ORTEP diagram of **14**. Taken from ref. [29], with permission from Elsevier.

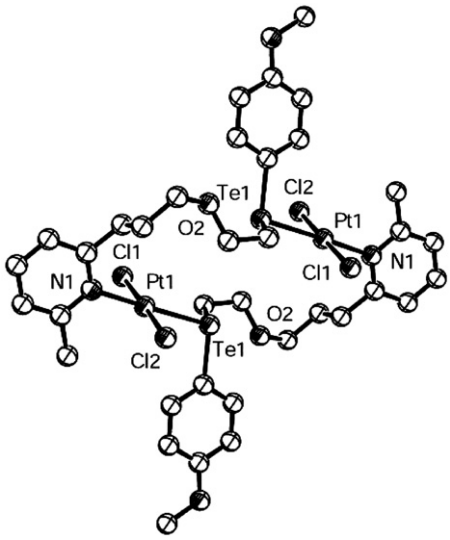

Fig. 11. ORTEP diagram of **15**. Taken from ref. [28], with permission from Elsevier.

lurium atoms of the ditelluroether, $MeTe(CH_2)_3TeMe$, participate in the formation of polymeric species $[Ag(MeTe(CH_2)_3TeMe]_n[BF_4]_n$.

Singh and coworkers have reported the synthesis of 20-membered metallomacrocycles (**14**, **15**) [28,29]. In these macrocycles, the Pd and Pt have a square planar geometry consisting of two *trans* Cl atoms along with the Te atom of one bridging ligand and the N atom of the other (Figs. 10 and 11).

5. Mixed donor (N/O/S/Te) macrocycles

5.1. Te/N macrocycles

An easy, high yield template free synthesis of novel tellurium azamacrocycles (**17–23**) with varying sizes (i.e. from 22 to 34) and donor atoms (from 6 to 10) are isolated *via* one step dipodal 2+2 condensation of bis(2-formylphenyl) telluride (**16**) with a series of diamines (Scheme 6) [30–34]. In these cases, the secondary intramolecular Te···N interactions play an important role in the formation of a macrocyclic ring by reducing the unfavorable lone pair–lone pair repulsion between the nitrogen atoms in the ring. The structures of **17** [30] and **23** [33] are similar and the macrocycles are puckered. Although there is an equal chance of N(1B) or N(2B#2) coordinating to the Te(2) atom in **23**, the N(1B) atom is not coordinated to Te(2) (Fig. 12). Thus, there is only one of two possible N–Te coordination bonds per tellurium atom and consequently, these macrocycles belong to 10-Te-3 tellurane structural type. Due to the fast (on NMR timescale) Te···N(1), Te···N(2) bond scrambling, NMR studies of the compounds in solution do not distinguish between the two topomeric 10-Te-3 structures and give very symmetric NMR spectra. Because of the Te···N interaction the geometry around each tellurium atom is T-shaped, a typical geometry for a 10-Te-3 tellurane [35].

The Schiff base macrocycle **17** forms a stable 1:2 complex **24** with $PdCl_2$ [30]. However, the complexation of **17** with another 'soft' Lewis acid, $HgCl_2$, shows a strange behavior. The reaction of **17** with $HgCl_2$ led to ring opening, resulting in the formation of a mixture of bis(organomercury) Lewis acid (**26a**) and bis(organotellurenyl chloride) (**26b**) (Scheme 7). This interesting dismutation reaction proceeds through the formation of a weakly associated addition complex **25** followed by the migration of groups.

The formation of 1:1 Pd(II) complexes of **17** (Scheme 7) [31,32] and **23** [33] is in contrast to the formation of the hydrolyzed product from the similar reaction of selena analogue [36]. The spectroscopic data and X-ray crystal structure (for **28**, Fig. 13) show that two nitrogen atoms (of the same diaminoethane unit) and two tellurium atoms are coordinated to the metal ion. The other two nitrogen atoms N(1C) and N(1D) are directed at the Pd center but are at largely nonbonding distances (4.152 and 4.134 Å) from the Pd center. The shorter Pd–Te bond distances are due to the soft–soft interactions. Here, the tellurium atoms not only act as donors to Pd but also act as acceptors to N and consequently act as Lewis acid and Lewis base. Interestingly, a similar reaction of **17** with $Pt(cod)Cl_2$ affords an unusual cleaved complex **29** (Scheme 7). This novel organoplatinum complex **29** results from a facile C–Te bond cleavage and transmetalation [31,32]. The facile cleavage of the C–Te bond is due to strong N–Te intramolecular interactions ($n \rightarrow s^*_{C-Te}$), which activate the *trans* C–Te bond. This strong intramolecular interaction is mainly due to the presence of the sp^2 nitrogen atom. In **29**, the Pt(II) is coordinated by carbon, tellurium and two nitrogen atoms in a square planar arrangement (Fig. 14). The cations are linked by intermolecular weak Te···Pt contacts to give dimers. This is the first example of a structurally characterized organoplatinum complex having both intramolecular Te–Pt and intermolecular Pt···Te interactions.

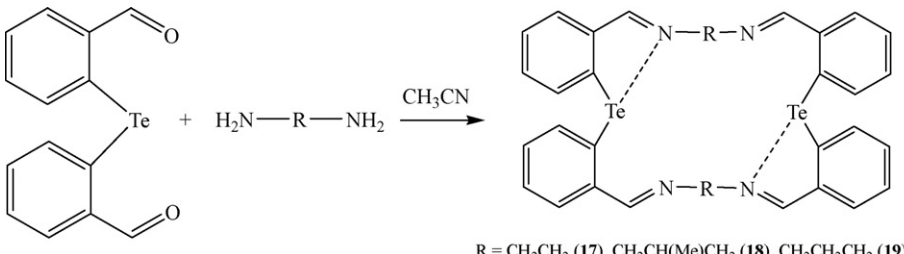

16

R = CH_2CH_2 (**17**), $CH_2CH(Me)CH_2$ (**18**), $CH_2CH_2CH_2$ (**19**), $CH_2(CH_2)_4CH_2$ (**20**), $CH_2CH_2NHCH_2CH_2NHCH_2CH_2$ (**21**), $CH_2CH_2NHCH_2CH_2$ (**22**) and trans-1,2-cyclohexanediyl (**23**)

Scheme 6.

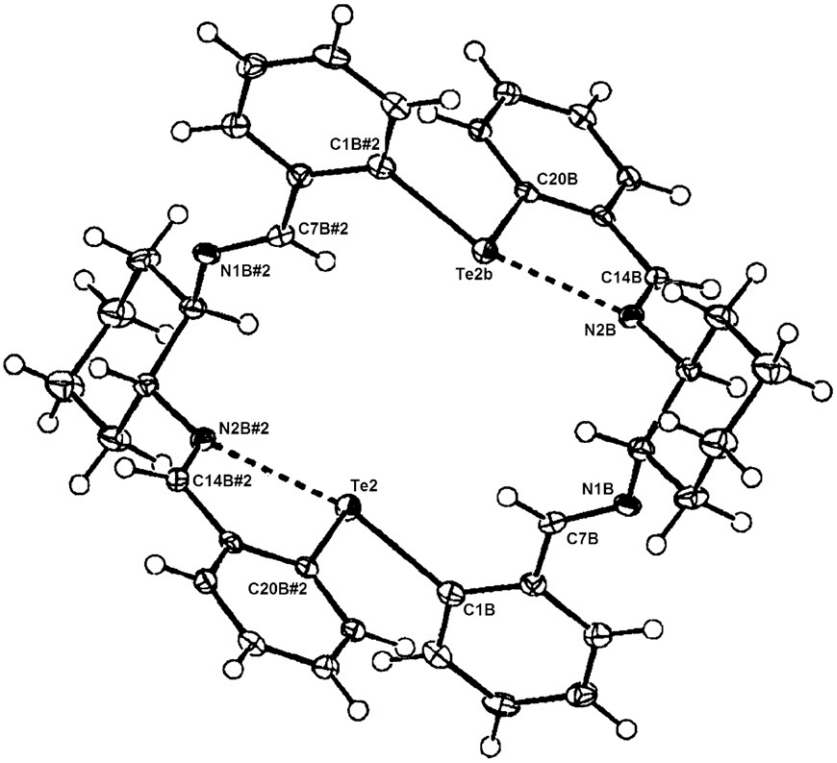

Fig. 12. Molecular structure of compound **23**. Taken from Ref. [33] with permission from the corresponding author. Copyright Wiley–VCH Verlag GmbH & Co. KGaA. Reproduced with permission.

Reaction of $NiCl_2{\cdot}6H_2O$ with **17** followed by the addition of excess of PF_6^- affords the air stable reddish brown Ni(II) paramagnetic complex **30** (Scheme 7) [31]. Similar bands in the UV/Vis spectra of solution and solid state indicate the presence of the same species in the solution as in the solid state. The structure shows that the Ni^{II} ion occupies the macrocyclic cavity and is bonded to all the six donor atoms (Te_2N_4) in a distorted octahedral arrangement (Fig. 15). Here, adaptability of **17** leads to a *cis*-disposition of Te donors. The hard-soft nature of Ni–Te bonding results in a Ni–Te mean bond distance 2.66 Å, longer than the sum of the single bond covalent radii of Ni(II) in octahedral environment (0.83 Å) and Te (1.37 Å).

These Schiff base macrocycles are prone to transmetallation and hydrolysis on treatment with metal salts (*vide supra*) leading to cleavage of the macrocycle [30,32,36,37]. The reduced form of the macrocycles with only sp^3 hybridized atoms are much more flexible and can accommodate a larger range of shapes and sizes than the parent Schiff base macrocycles that have sp^2 hybridized donor atoms. The large upfield shifts of $^{77}Se/^{125}Te$ NMR for reduced macrocycles compared to the parent Schiff base macrocycles and single crystal X-ray structure [38] show a weaker E···N interactions in the former. So, to synthesize stable complexes of telluraaza macrocycles, reduction of **17** is undertaken (Scheme 8).

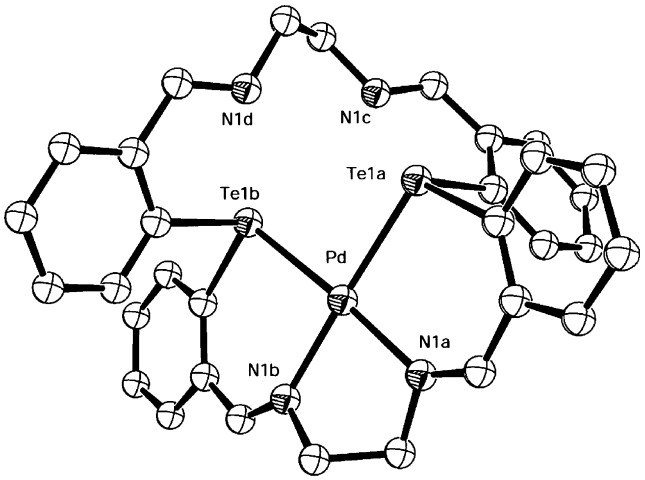

Fig. 13. An ORTEP diagram of **28**. Taken from Ref. [32]. Reproduced by permission of The Royal Society of Chemistry.

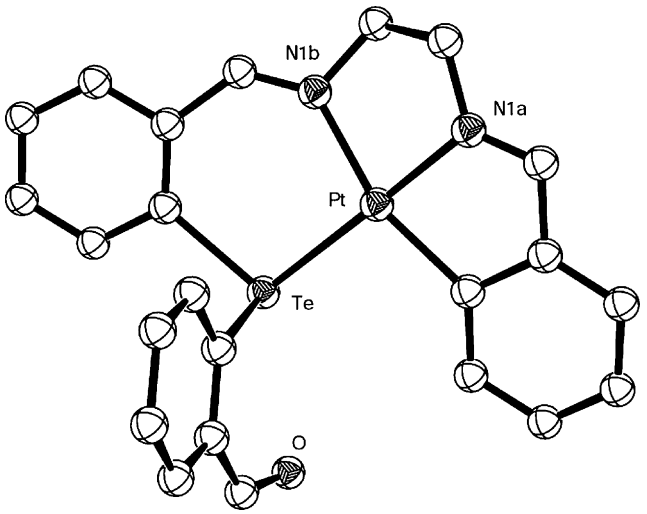

Fig. 14. An ORTEP diagram of Pt complex **29**. Taken from Ref. [32]. Reproduced by permission of The Royal Society of Chemistry.

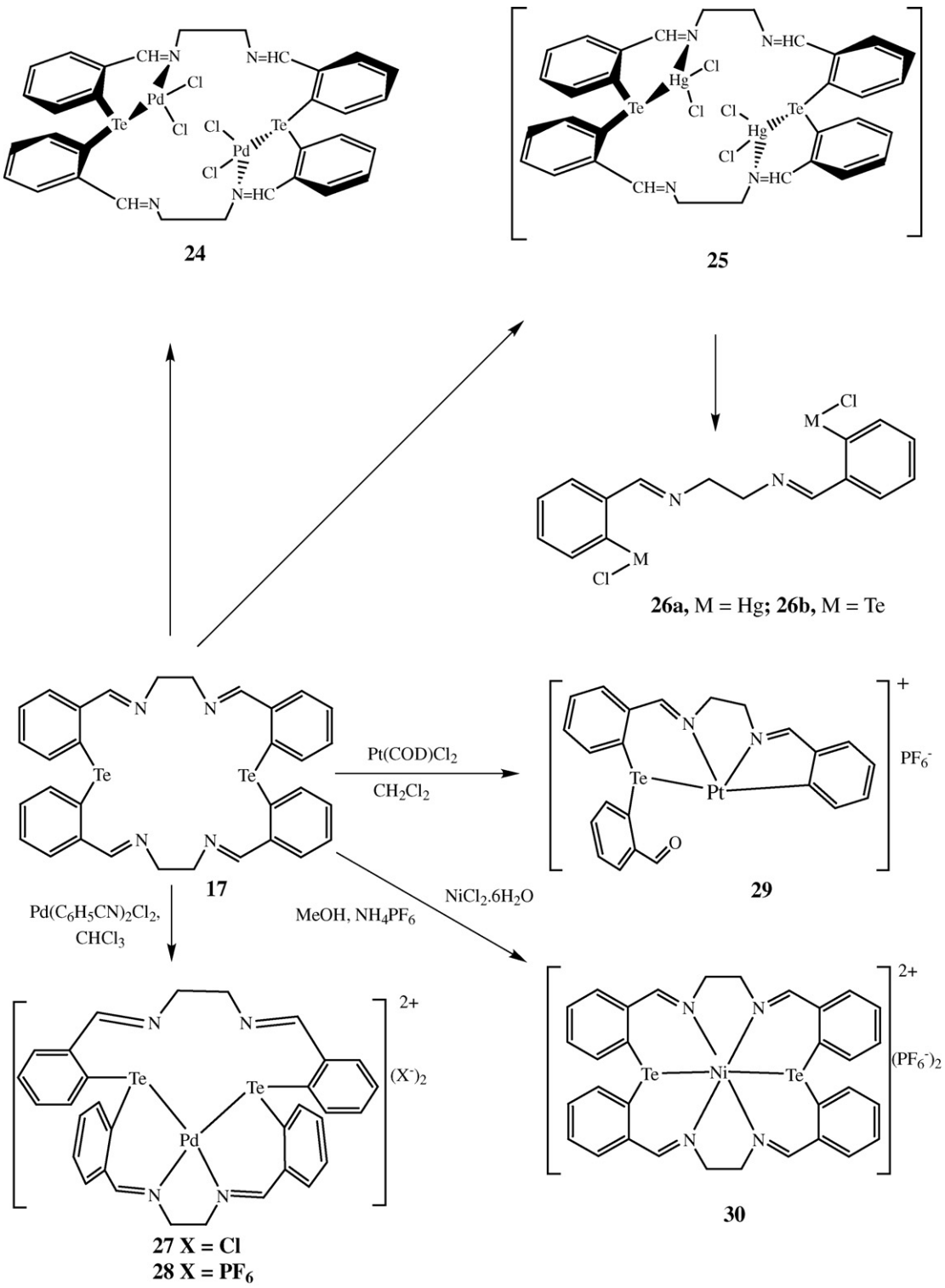

Scheme 7.

The reaction of **31** with Pd(II) gives the desired 1:1 complex **32** [37,38]. The molecular structure of **32** (Fig. 16) shows coordination of two nitrogen and two tellurium atoms to Pd(II) similar to the parent Schiff base macrocycle Pd(II) complex **28**. The remaining two nitrogen atoms are at nonbonding distances (3.653 Å for N1B and 4.753 Å for N2B). However, the molecular structure of the Pd(II) complexes of the corresponding 22-membered selenaaza macrocycle shows coordination of only hard N donor atoms to Pd(II) [37,38]. This anomalous behavior is due to the greater σ-donor property of the Te over Se leading to a strong soft-soft interaction and stabilization of the 6-membered chelate ring. The intramolecular Te···N bonds (2.8 Å), which decreases the electron-donor activity of the N atom, can cause a decrease in the number of active donor sites in this ligands. The packing diagram shows that the water molecules

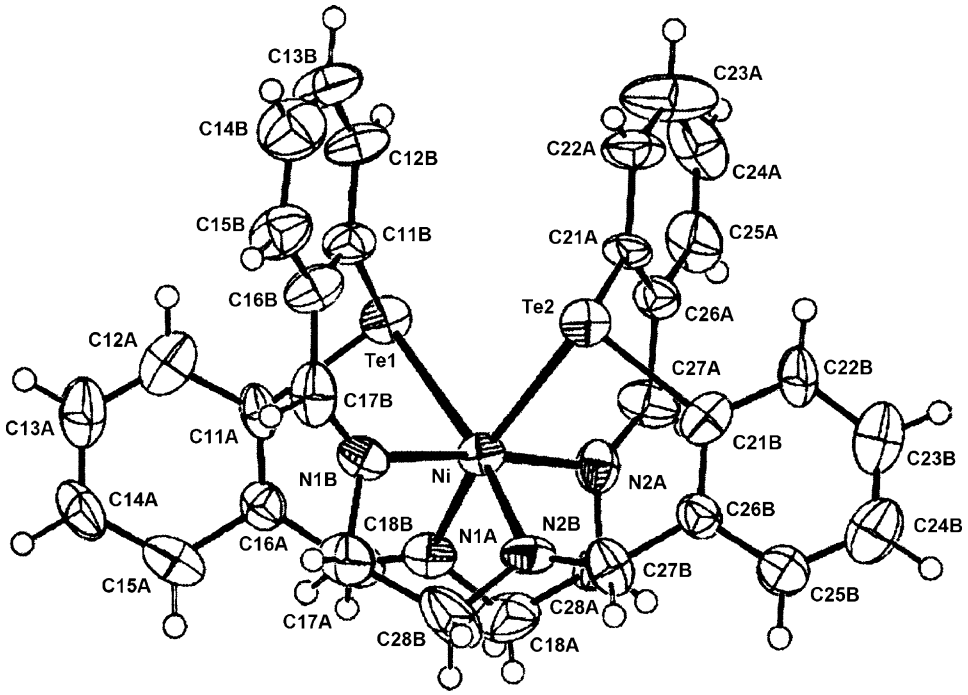

Fig. 15. An ORTEP diagram of **30**. Taken from Ref. [31]. Copyright (2004). With permission from Elsevier.

are sandwiched between the complexes and that there is extensive hydrogen bonding between the N–H hydrogen atom, chloride counter ion and the water molecules.

The protonated derivative **33** [30] is obtained as depicted in Scheme 8. The crystal structure of **33** shows that none of the bromide counter ions are situated inside the macrocyclic cavity, but one lies above the macrocycle and forms intermolecular hydrogen bonding with the amine and water hydrogen atoms [31]. All the four nitrogen atoms are not in the same plane and the macrocycle is highly puckered (Fig. 17). The intramolecular Te···Te distance (7.108 Å) is greater than the corresponding distance (4.979 Å) in the parent Schiff base **17**.

The 24- and 28-membered macrocyclic Schiff type ligands **34** with O, N and Te donor sets are isolated *via* template free (2+2) condensation reactions of bis(aminoalkyl)tellurides, $\{NH_2(CH_2)_n\}_2Te$ (n = 2 or 3) with 2,6-diacetyl-4-methylphenol [39]. The octahedral Mn(II), Co(II), Ni(II), Cu(II) and Zn(II) complexes of a tellurium containing tetraazamacrocycle are accounted [40].

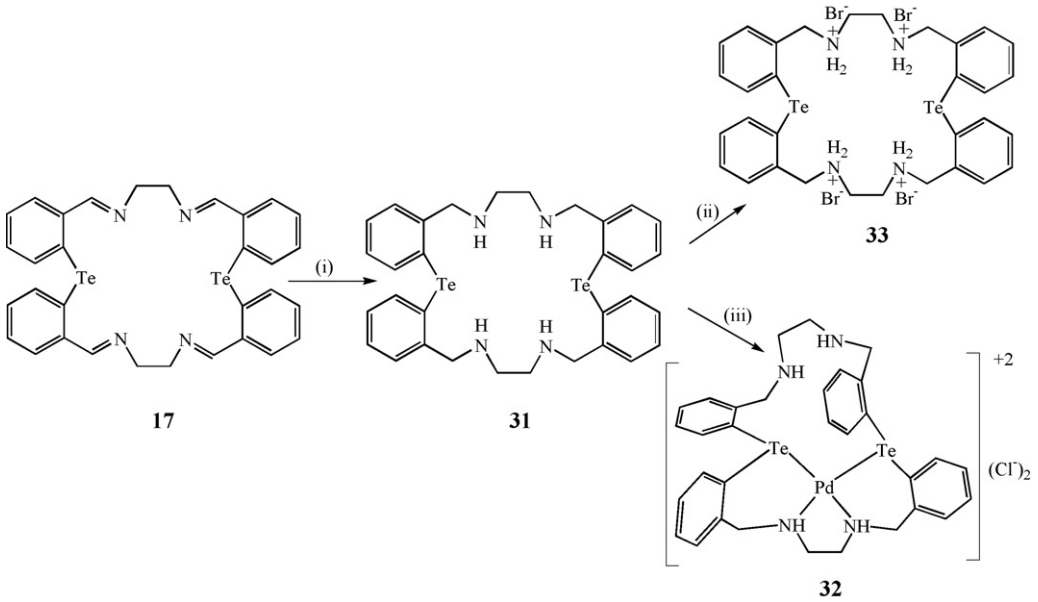

Scheme 8. (i) $NaBH_4$, MeOH; (ii) 48% HBr, EtOH; (iii) $PdCl_2$, MeOH (reflux).

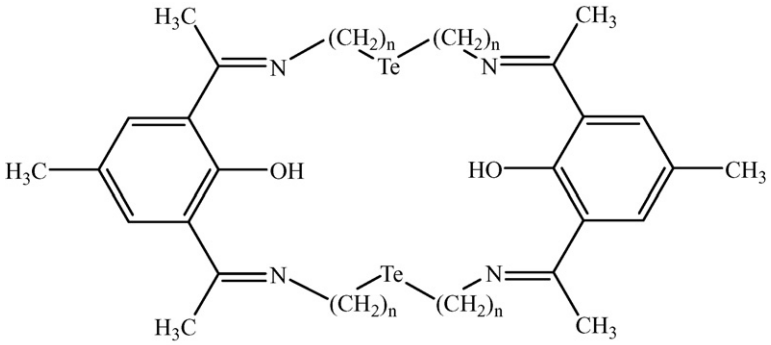

34

In summary, the Schiff base macrocycles belong to 10-Te-3 structural type. The compounds posses a slightly distorted T-shaped configuration at the tellurium centers with two lone pair electrons formally occupying equatorial positions of its ψ-trigonal bipyramidal coordination polyhedron. From a comparison of E···N (E = Se or Te) bond lengths in Schiff base macrocycles and its reduced form with identical substituents at the chalcogen centers and differently hybridized nitrogen atoms, it follows that the intramolecular coordination bond of E–N_{sp3} type are weaker than those of the E–N_{sp2} type. This conclusion is supported by $^{77}Se/^{125}Te$ NMR studies in solution. The Schiff base macrocycle shows versatile coordination behavior but are prone to transmetalation with Pt(II) and Hg(II) cations leading to cleavage of the macrocycle. The formation of the desired 1:1 Pd(II) complex of **17** is contrast to the formation of hydrolyzed product with Se-analog. The more flexible reduced Schiff base macrocycle **31** behaves as an N2Te2 donor ligand towards Pd(II) cation whereas in selena analog only nitrogen atom coordinate to Pd(II). This shows the greater σ-donor property of Te over Se. The X-ray crystal structures of **28** and **32** reveal only N2Te2 coordination to the metal out of the possible N4Te2 donor sets in the ligands; the other two nitrogen atoms remaining at large nonbonding distances. One of the reasons for this decreased dentacity of the ligands is the formation of intramolecular Te–N bonds, which, in turn, decrease the electron-donor activity of the N atoms. The protonated derivative **33** should recognize the anions.

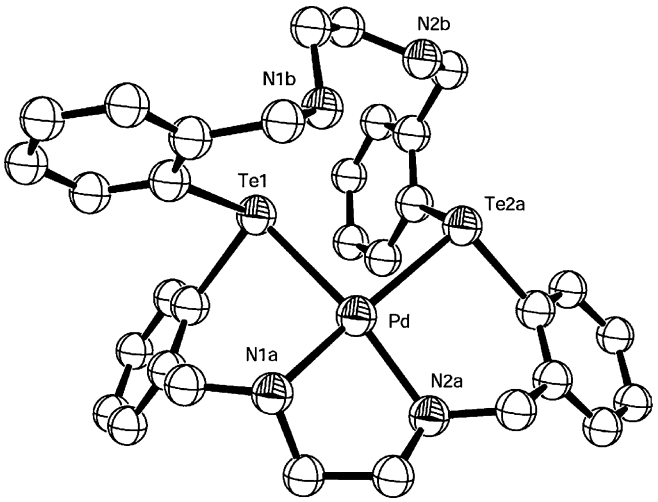

Fig. 16. Packing diagram of **32**. Taken from Ref. [38]. Copyright Wiley-VCH Verlag GmbH and Co. KGaA. Reproduced with permission.

5.2. Te/O macrocycles

The ligand 4′-(2-pyridylmethyleneamino)benzo-10-tellura-15-crown-5 (dic-Te) is synthesized modifying the procedure reported for (2-pyridylmethyleneamino)benzo-15-crown-5 (dic) [41]. The photophysics and electrochemistry of the copper(I) diimine complex, $[Cu(PPh_3)_2(dic\text{-}Te)]BF_4$ (**35**), have been studied [42]. Unlike

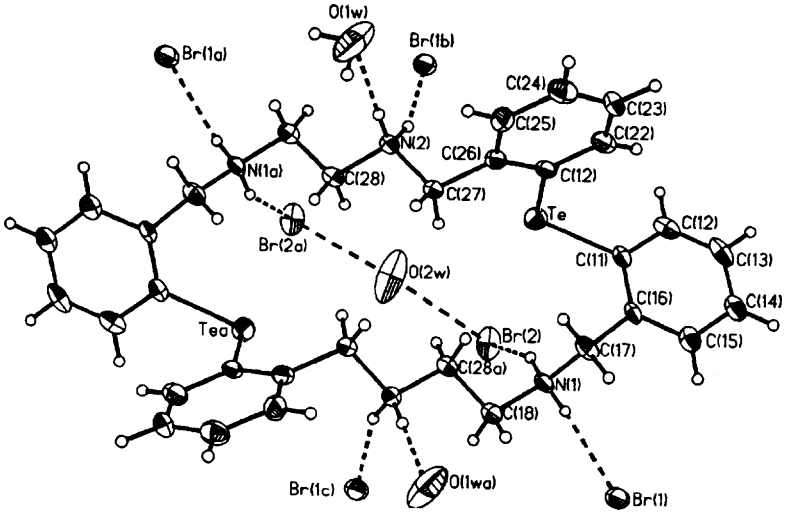

Fig. 17. An ORTEP diagram of **33**. Taken from Ref. [31]. Copyright (2004). With permission from Elsevier.

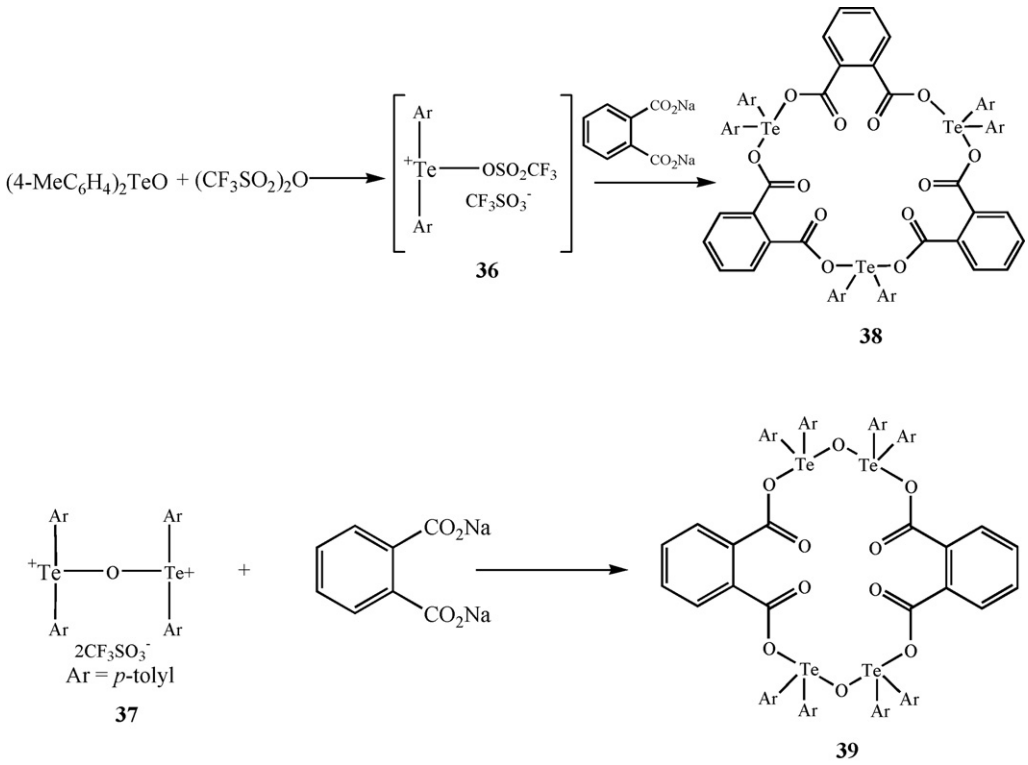

Scheme 9.

$[Cu(PPh_3)_2(dic)]BF_4$, which preferentially binds to alkali and alkaline earth metal ions (such as Na^+, K^+ and Ba^{2+}), (**35**) binds to softer metal ions such as Zn^{2+} and Cd^{2+} due to the soft Te donor atom despite the similar radius of Cd^{2+} and Na^+. So, in this system, the hard–soft acid–base factor governs the ion binding properties instead of size-match selectivity.

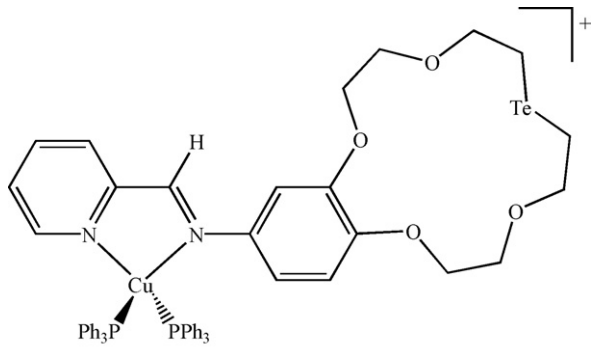

35

Kobayashi and coworkers reported the synthesis of the macrocyclic multi-telluranes **38**, a 21-membered ring and **39**, an 18-membered ring (Scheme 9) [43]. This is the first example of macrocycles composed of only hypervalent Te–O apical linkages in the main chain for group 13–17 elements. Hypervalent bonds *via* $n \rightarrow \sigma^*$ orbital interactions in heteroatoms can serve as a new supramolecular synthon for molecular assembly. The molecular structures of these macrocycles show distorted trigonal bipyramidal geometries for the Te atoms with hypervalent Te–O apical bonds. The lone pair is stereochemically active and distorts the O–Te–O and C–Te–C angles. The macrocycle **38** (Fig. 18) is composed of three Te atoms and three pthalates whereas the macrocycle **39** consists of two ditelluroxanes and two phthalates. In both cases, all the atoms of the respective macrocyclic rings are roughly coplanar. The compound **39** forms a head-to-head type of dimeric structure in the solid state because of the interaction of tellurium atoms and the carbonyl oxygen atom of the adjacent molecule. The Te(IV) cations in **38** are arranged in an equilateral triangular fashion with no interaction between the intramolecular tellurium atoms similar to **12**.

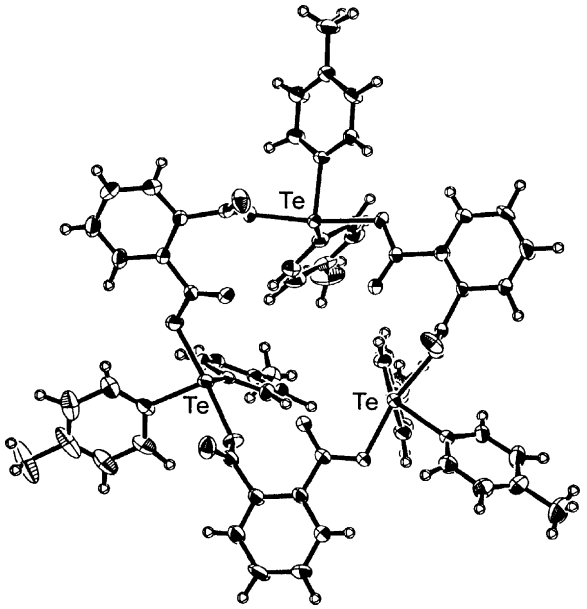

Fig. 18. Crystal structure of **38**. Taken from Ref. [43]. Reproduced by permission of The Royal Society of Chemistry.

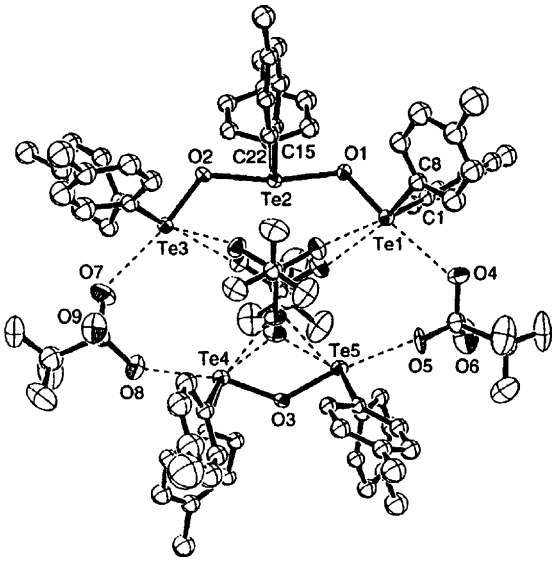

Fig. 19. Crystal structure of $[C_6H_4\text{-}4\text{-}Me)_2\text{–}Te\{OTe(C_6H_4\text{-}4\text{-}Me)_2\}_2][Te(C_6H_4\text{-}4\text{-}Me)_2OTe(C_6H_4\text{-}4\text{-}Me)_2][CF_3SO_3]_4$ (**40**). Taken from Ref. [44]. Copyright Wiley-VCH Verlag GmbH and Co. KGaA. Reproduced with permission.

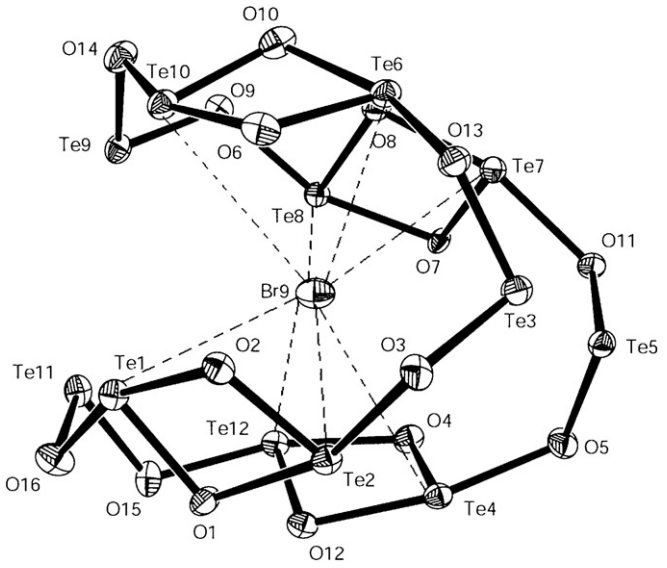

Fig. 20. Labeling scheme of the $Te_{12}O_{16}$ skeleton and the central bromine anion of the $[\{(Pr^iTe)_{12}O_{16}Br_4\{Li(THF)Br\}_4\}Br]^-$ anion. Taken from Ref. [45]. Reproduced by permission of The Royal Society of Chemistry.

Kobayashi and coworkers have reported the formation of a 14-membered pseudoring, **40**, from the congregation of cationic ditelluroxane $[Te(C_6H_4\text{-}4\text{-}Me)_2OTe(C_6H_4\text{-}4\text{-}Me)_2]^{2+}$ and tritelluroxane $[C_6H_4\text{-}4\text{-}Me)_2\text{–}Te\{OTe(C_6H_4\text{-}4\text{-}Me)_2\}_2]^{2+}$ by interaction of their terminal Te atoms with two triflate counterions in the solid state [44]. The other two counterions are accommodated in the cavity of the macrocycle (Fig. 19). Te(IV) in **40** has a pseudo trigonal bipyramidal geometry with hypervalent apical Te–O bonds and all the atoms of this ring are coplanar, similar to that observed in compounds **38** and **39**. Lone pair occupies the site generally presumed to be the lone-pair region in trigonal-bipyramidal AB_4E molecules [20].

A novel 'telluroxane' $[Li(THF)_4][\{Pr^iTe)_{12}O_{16}Br_4\{Li(THF)Br\}_4\}Br]$ containing a $Te_{12}O_{16}$ ring was obtained as a partial air oxidation product of a mixture of lithium hex-1-ynyl tellurolate and isopropyl bromide in THF [45]. The novel tellurium oxide cage compound exhibits the remarkably rare property of spherically encapsulating a bromide anion in its cavity which is stabilized by four Li(THF)Br units and four bromide anions in an outer shell. The capability of entrapping an atomic size guest in its cavity makes it a promising candidate for a variety of applications in chemistry [45]. Crystals of the macrocycle consist of isolated $[Li(THF)_4]^+$ cations, $[\{Pr^iTe)_{12}O_{16}Br_4\{Li(THF)Br\}_4Br]^-$ anions and uncoordinating solvent molecules. The macrocycle of alternating tellurium and oxygen atoms forms from the head-to-tail attachment of four O–Te–O–Te(μ-O)$_2$Te-monomers (Fig. 20). The four Te(μ-O)$_2$Te microcycle connect to the –OTeO– building block by weak Te–O-interactions, while the O–Te–O unit itself contains stronger Te–O bonds. The encapsulated bromide anion is located inside the cavity with four long and eight short Br(9)–Te distances. Stabilization of the spherical $Te_{12}O_{16}$ framework is provided by the nine bromide anions, one inside and eight outside the sphere. The eight tellurium atoms of the Te(μ-O)$_2$Te microcycle have weaker interactions to the central Br(9) compared to the stronger interactions to the 'outer' bromine atoms. Stronger Te–Br interactions occur between the O–Te–O building blocks and 'outer' bromide anions.

The novel macrocycle 1,10-ditellura-4,7,13,16-tetraoxacyclooctadecane (**18O4Te2**) is prepared from Na_2Te and $ClCH_2(CH_2OCH_2)_2CH_2Cl$ by Levason and coworkers [46]. 1-Tellura-4,7-dioxacyclononane (**9O2Te**) is the minor by-product of the reaction. The Te(IV) derivatives **18O4Te2Me$_2$I$_2$**, **18O4Te2Cl$_4$** and **9O2TeMeI** are prepared to characterize the macrocycle. The Pd(II) and Pt(II) complexes of **18O4Te2** $[MLX_2(MeCN)_2]$ (X = Cl or Br) are isomorphous. The spectroscopic, NMR and X-ray studies show the *cis* geometry and the non-interaction of ethereal oxygen atoms. In both the cases, **18O4Te2** behaves as a bidentate Te2 chelating ligand to the metal ions forming two 11-membered rings. The structures show *cis* square planar geometry in which the soft–soft palladium/platinum–tellurium interactions occur according to the HSAB principle (Fig. 21). The longer Pt–Cl bond distances compared to its thia and selena analogues shows the greater *trans* influence of Te over Se and S.

Several other complexes of **18O4Te2** have been reported including $[RhCl_2L_2]Y$ (Y = Cl, PF_6), $[CuL_2]BF_4$, $[AgL_2]BF_4$ and $[Cu_2L][BF_4]_2$. The Pd and Pt complexes of **9O2Te** of the type $[MCl_2\{\mathbf{9O2Te}\}_2]$ are also known [46].

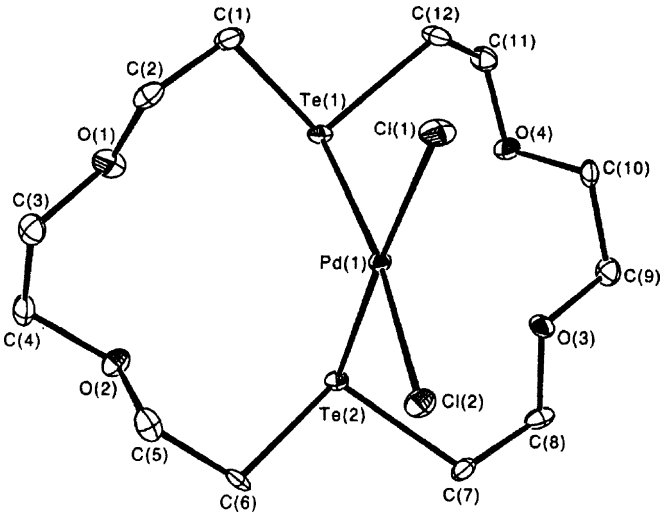

Fig. 21. Crystal structure of $[PdCl_2$**18O4Te2**$]$. Taken from Ref. [46]. Reproduced by permission of The Royal Society of Chemistry.

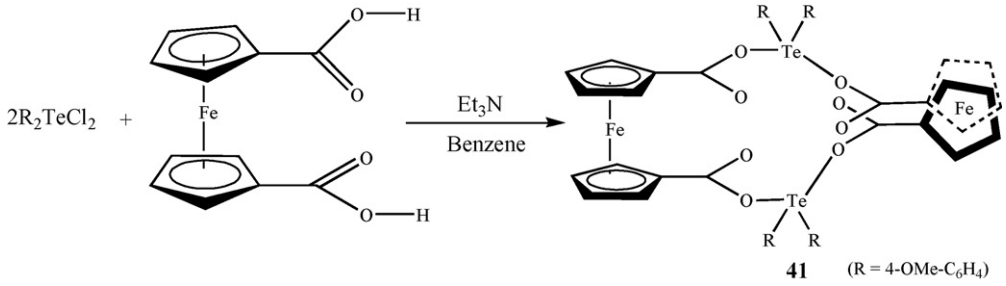

Scheme 10.

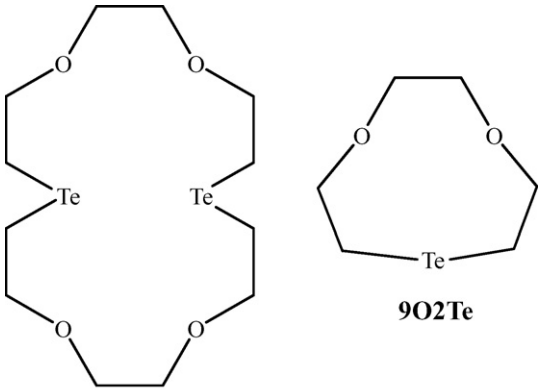

18O4Te2

The reaction of 1,1′-ferrocenedicarboxylic acid, LH_2, with Ar_2TeCl_2 (Ar = 4-OMe-C_6H_4) in the presence of triethylamine afforded 16-membered heterobimetallic tetranuclear macrocycle $[Ar_2TeL]_2$ (**41**) (Scheme 10) [47]. The primary geometry of the tellurium in this compound is ψ-trigonal bipyramid with the oxygen atoms taking the axial positions and the organyl groups and the stereochemically active lone pair of electrons being equatorial (Fig. 22). The O–Te–O angle substantially deviates from the ideal 180°. The larger space requirement of the lone pair is also indicated by the Ceq-Te-Ceq angle being smaller than 120° and the tilt of the axial chlorine towards equatorial one. The two ferrocene ligands in this macrocycle are nearly orthogonal to each other (88.2°). This macrocycle represents the first example of a structurally characterized organotellurium compound containing ferrocene ligands. Cyclic voltammetric study of **41** showed two quasi-reversible single electron oxidations. Based on the comproportionation constants ($K_c \sim 10^2$), following Robin–Day classification [48], the compound **41** is placed in an intermediate class between non-coupled and weakly coupled systems, in which the ferrocene groups are substantially non-communicating.

Novel tellura crown ethers are synthesized from the reaction of bis(2-hydroxyethyl)telluride with diol ditosylates. The platinum complex of 10-tellurabenzo-15-crown-5 is reported therein [49]. The catalytic activity of the platinum complex of the novel 2,3-benzo-1,4,7,13-tetraoxa-10-telluracyclopentadeca-2-ene is studied for the hydrosilylation of olefins by triethoxysilane [50]. Some other novel crown ether possessing tellurium atoms are also known [51,52].

The first organotellurium(IV) chelates of the type $R_2TeSalen$ were reported in 1982 [53]. Recently the single crystal structure of one of these chelated complexes [(*p*-MeO-Ph)$_2$Te(salen)] (**42**) where the Te(IV) binds to only two oxygen donor atoms of the salen ligand has been re-examined. The two nitrogen atoms are at largely nonbonding distance from the Te center. The electron pair arrangement about Te(IV) is ψ-trigonal bipyramidal geometry as expected for AX_4E system on the basis of VSEPR theory (Fig. 23). The salen oxygen atoms occupy axial positions and the two ani-

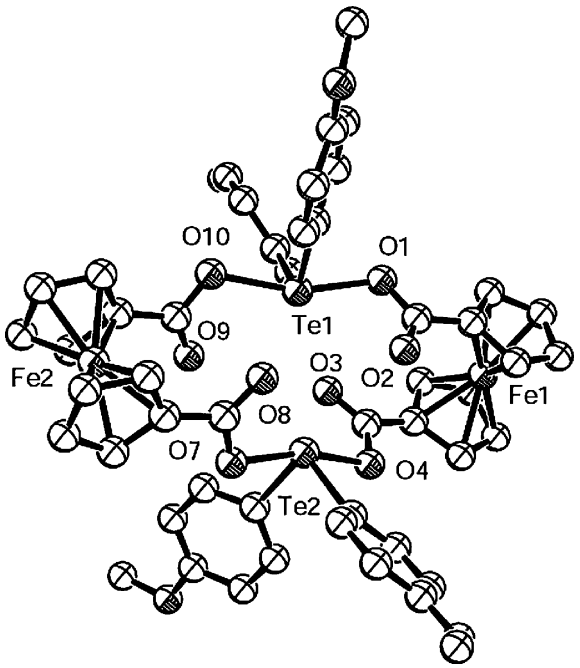

Fig. 22. ORTEP diagram of **41**. Reprinted with permission from [47]. Copyright (2007) American Chemical Society.

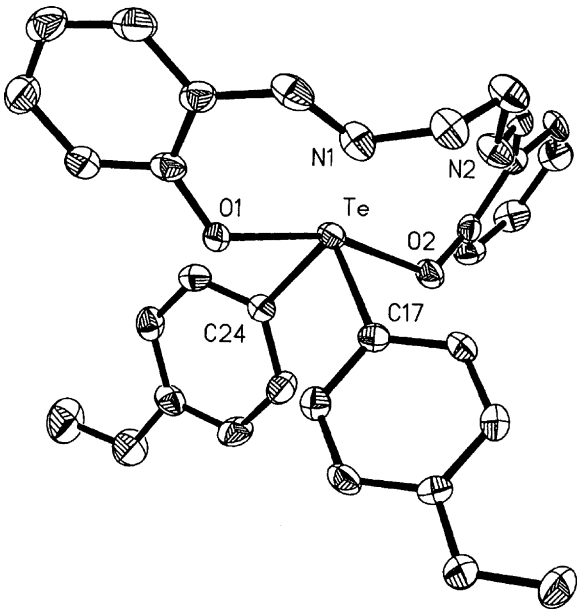

Fig. 23. ORTEP diagram of **42**. Taken from Ref. [54].

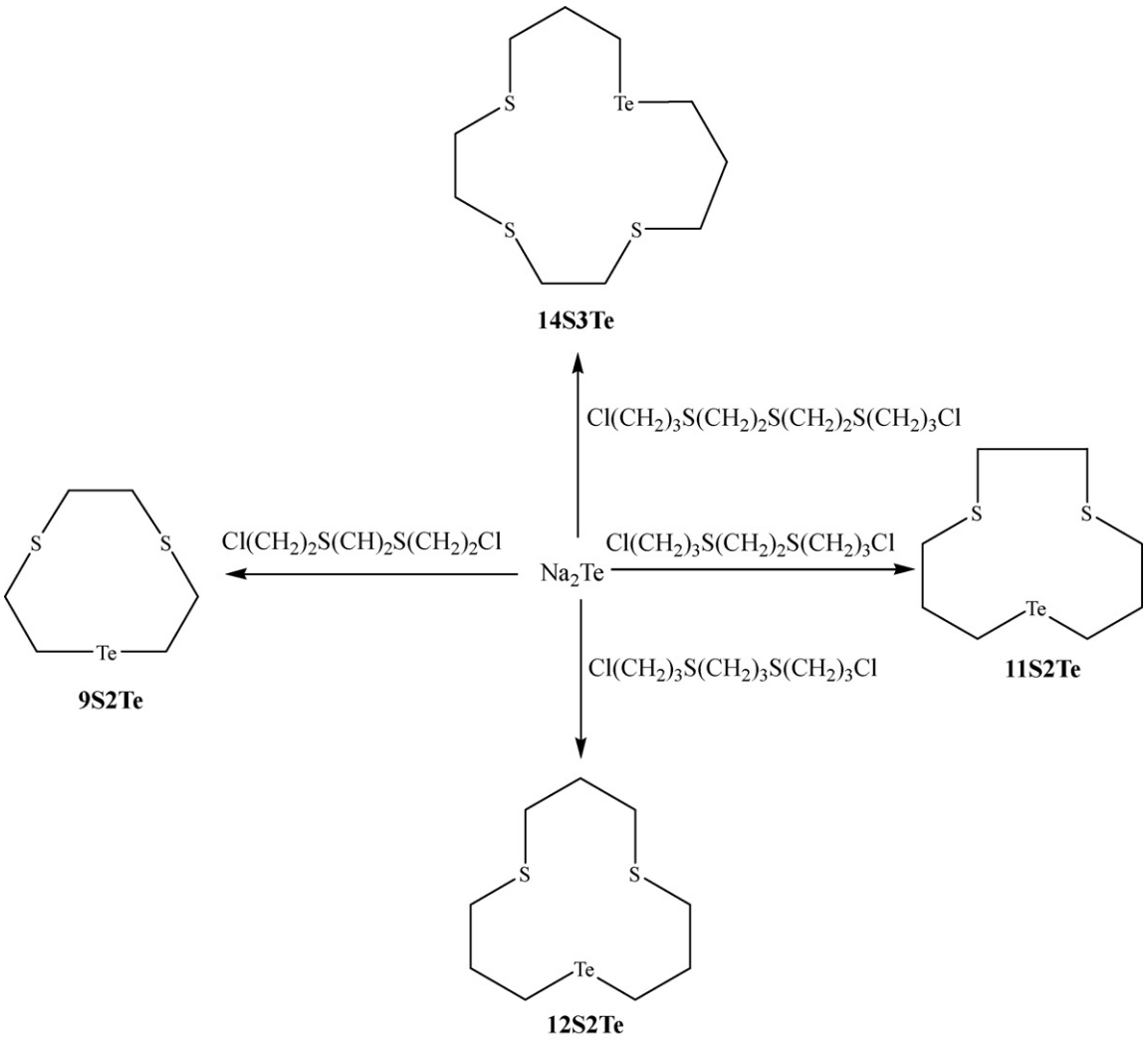

Scheme 11.

syl carbon atoms and the lone pair occupy the equatorial sites [54]. Both axial and equatorial ligands are bent away from the vacant site to reduce the lone pair–bonding pair interactions. The deviations of the angles around Te in **42** is similar to the deviations observed for Te(IV) with apical oxygen atoms in **38–41** (*vide supra*).

5.3. Te/S macrocycles

Four new mixed S/Te-donor macrocycles of different ring sizes were prepared from [1+1] cyclization of Na_2Te and the corresponding α,ω-dichlorothioalkane with no evidence of the formation of [2+2] products (Scheme 11) by Levason and coworkers [55–57]. This is unlike the formation of the [2+2] cyclization product as major one in an analogous reaction of Na_2Te and $Cl(CH_2)_2O(CH_2)_2O(CH_2)_2Cl$ [46]. A ring contraction product, 1-thia-4-tellura-cyclohexane, is observed as by-product from the preparation of $9S_2Te$. The crystal structure of **11S2Te** (Fig. 24) and **12S2Te** (Fig. 25) shows the explicit formation of the [1+1] cyclization products and discrete molecular species, with no significant intermolecular contacts. The structure of **12S2Te** is very similar to that of the related trithia crown, **12S3**, which adopts an approximately square arrangement with one S atom at a corner and the other two S atoms on edges [58]. Compound **11S2Te** shows a similar conformation with the Te atom on a corner and the S atoms on edges. The smaller C–Te–C angles compared to the C–S–C angles (Table 1) show greater stereochemical activity of the lone pairs in the later consistent with the decrease of stereochemical activity of lone pair with increasing period number of central atom within a chemical group.

The more stable organo-Te(IV) methiodide derivatives for all the three S2Te-donor macrocycles and the Te(IV) diiodide species **11S2TeI$_2$** and **12S2TeI$_2$** are also reported therein. The structure of

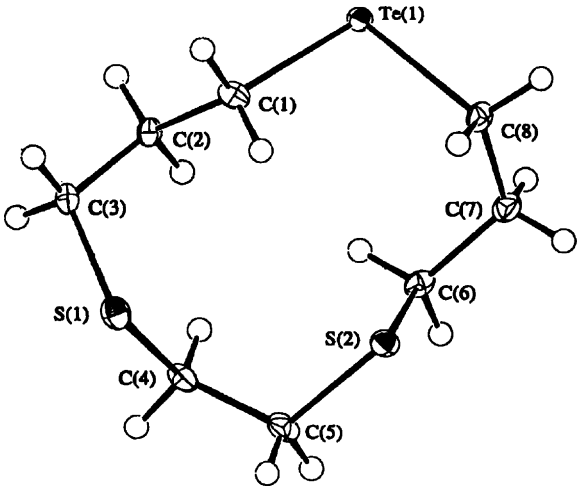

Fig. 24. Crystal structure of **11S2Te**. Taken from Ref. [56]. Reproduced by permission of The Royal Society of Chemistry.

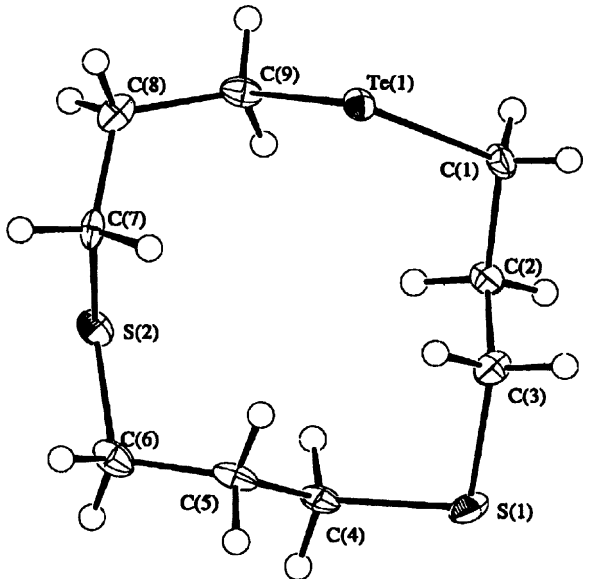

Fig. 25. Crystal structure of **12S2Te**. Taken from Ref. [56]. Reproduced by permission of The Royal Society of Chemistry.

12S2TeI$_2$ shows distorted pseudo trigonal bipyramidal geometry at Te(IV) typical of R_2TeX_2 species, having two *trans* iodine atoms while the carbon atoms and non-bonding pair electrons on tellurium occupy the equatorial plane [56]. The ring adopts a similar conformation to that of the parent macrocycle except that the Te atom occupies a corner position rather than a S atom (Fig. 26).

The coordination chemistry of these macrocycles is studied with a range of transition metal ions. The macrocycles form complexes with Ag(I) of the type [Ag***n*S2Te**]$^+$ (n = 11 and 12) and [Ag(***n*S2Te**)$_2$]$^+$ (n = 9, 11 and 12). The crystal structure of [Ag**11S2Te**]BF_4 (Fig. 27) complex shows a one-dimensional polymeric structure [55]. The Ag(I) ions adopt a distorted trigonal planar coordination environment *via* two S and one Te atom from three different macrocycles. Polymeric structures for the other Ag(I) species are predicted.

The related 1:1 species [Cu***n*S2Te**]BF_4 (n = 11 or 12), the Pd(II) and Pt(II) complexes [MCl_2***n*S2Te**] (n = 11 or 12) and the distorted octahedral Rh(III) species [Rh(Cp*)***n*S2Te**]$(PF_6)_2$ (n = 9, 11 or 12) are also reported [56]. The Mn(I) species *fac*-[Mn(CO)$_3$***n*S2Te**]CF_3SO_3 (n = 9, 11, 12) and the Mo(0) complex *cis*-[Mo(CO)$_4$**11S2Te**] have also been reported in the paper. Attempts to prepare analogous Mo(0) complex of the 9- and 12-membered rings were unsuccessful.

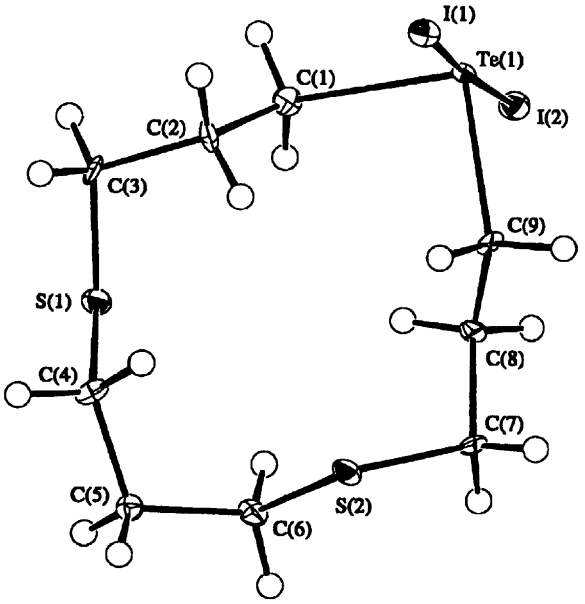

Fig. 26. Crystal structure of **12S2TeI$_2$**. Taken from Ref. [56]. Reproduced by permission of The Royal Society of Chemistry.

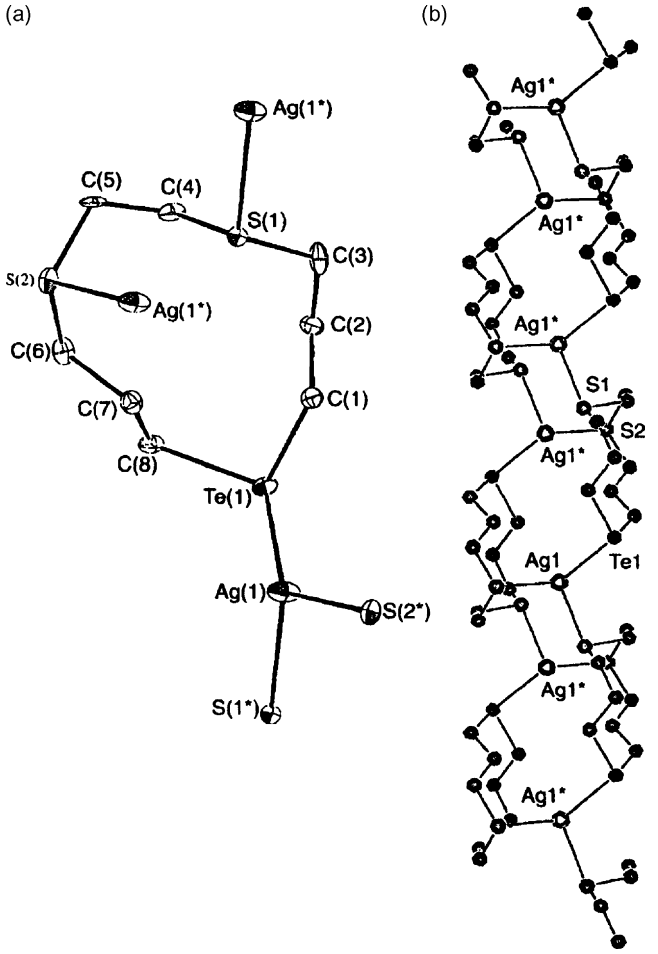

Fig. 27. Crystal Structure of (a) [Ag(**11S2Te**)]$^+$(BF_4^- salt). (b) View of a portion of the one-dimensional lattice adopted by [Ag(**11S2Te**)]BF_4. Taken from Ref. [55]. Reproduced by permission of The Royal Society of Chemistry.

6. Cryptand

The only known tellurium-containing cryptand (**43**) was synthesized from the [2+3] condensation of tris(2-aminoethyl)amine (tren) and bis(*o*-formylphenyl)telluride using cesium ion as template [59].

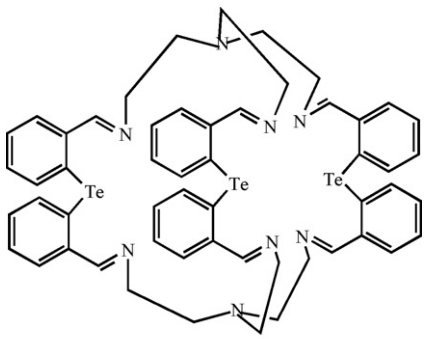

43

7. Comparisons of X-ray crystal structures

The primary geometry of Te(II) in the macrocycles with two covalently bonded substituents and two lone pairs of valence electrons is bent. The Schiff base macrocycles belong to 10-Te-3 structural type with T-shaped configuration at the tellurium center. The intramolecular Te···N interaction is substantially stronger in the case of Te(II) compounds than those compounds where tellurium is in a higher oxidation state Te(IV).

Comparisons of the structures of tellurium in +4 oxidation states are much more interesting due to the variations of the stereochemical activity of the lone pair of electrons. A tetravalent group 16 atoms with five electron pairs should arrange themselves in a trigonal bipyramidal manner. Since the non-bonding electron pair occupies more space around the central atom than the bond pairs, it is expected to occupy an equatorial position and deform the molecule in such a way that the bond pairs are pushed away [60]. This is indeed the kind of distortion that is observed. Tellurium in the hypervalent +4 formal oxidation states in the macrocycles are of the AB2B2′E type and have distorted pseudo-trigonal-bipyramidal (pseudo-tbp) geometry typical of R_2TeX_2 species. The most electronegative ligands, which have smallest bonding electron pairs, are in the usual axial positions. These compounds are commonly referred to as 10-E−4 systems (for the N-X-L formalism see [61]) indicating that the tellurium atom is formally associated with five pairs of electrons, only four of which are bond pairs (Fig. 28). The chemical bond in the axial-Te-axial fragment can be described using 3c–4e bonding system, which implies a total bond order of 1 (0.5 bond order for each Te-axial bond in symmetrical systems).

The stereochemical activity of the lone pair varies among the Te(IV) compounds. The stereochemically inactive lone pair remains in a spherically symmetrical orbital around the central atom and has little or no influence on the geometry of the molecule. When the lone pair has some p character, it tends to occupy a larger space in the coordination sphere, it causes some distortion from the ideal symmetrical structure as seen in the valence shall electron pair repulsion theory. This means that the lone pair is stereochemically active. The smaller axial–Te–axial and C_{eq}–Te–X bond angles in case of **8**, **38–42** compared to **12** and **12S2TeI$_2$** (Table 1) suggest a larger stereochemical influence of the non-bonding pair of electrons in the former than the latter. The structural distortion of Te(IV) atom in **8** can be attributed to the stereochemical activity of the lone pair along with the steric rigidity. The congestion about the central Te atom owing to the presence of chloro ligands and intramolecular Te···N secondary bonding appears to be responsible for steric rigidity. Longer Te–Cl bonds in **8** reduce the steric congestion. The structures about Te(IV) in **12** and **12S2TeI2** are similar and the angles around Te centers in **12** and **12S2TeI2** are comparable to those in Me_2Cl_2Te [62] and Me_2I_2Te [63] respectively with no influence of the ring structures (due to the *exo* positions of Te) on the geometry of the Te(IV). The lesser stereochemical activity of the lone pair electrons in these cases can be seen from the slight deviations of the X–Te–X and X–Te–C bond angles (Table 1) from ideal 180° and 90° respectively. Also slight lengthening of the Te–Cl and Te–I bonds (Table 1) in **12** and **12S2TeI2** respectively shows stereochemical ineffectiveness of the valence electron pair which remains in a spherically symmetrical 5s orbital around Te atom and thus shielding the bonding electron pairs from tellurium. The intermolecular Te···Cl bonds arising from the donation of the chlorine lone-pair density to an empty orbital (σ*) on more electropositive tellurium increase the coordination number for the tellurium atom and hence decrease the stereochemical activity of the lone pair in **12**. The decrease in stereochemical effectiveness of the lone pair in **12S2TeI2** is due to the bulky iodine atoms consistent with the fact that the stereochemical effectiveness of the free electron pairs in the halides of tellurium decreases in the direction $TeCl_n > TeBr_n > TeI_n$ (space required by the ligands increases).

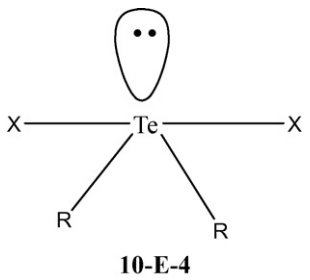

10-E-4

Fig. 28. Schematic representation for 10-E−4 hypervalent tellurium compounds.

Geometries of the Te(IV) in **38–42** with more electronegative donor atoms O, that are part of the macrocycles, substantially deviate from the ideal trigonal bipyramidal geometry due to the stereochemical activity of the lone pair electrons. The larger space requirement of the lone pair is indicated by the smaller C–Te–C angles in **38–42** than **12** and **12S2Te2I2** and the tilt of the axial ligands towards equatorial ones. Further distortions of molecular geometry in these compounds are caused by the steric demands of the ligands attached to the central atom. The observations made herein are consistent with the analysis of stereochemical activity of $6s^2$ lone pair of Pb(II) complexes using ab initio molecular orbital optimizations by Glusker and coworkers [64]. It is observed that Pb(II) complexes with coordination numbers from 6 to 8 are holodirected (stereochemically inactive lone pair) with large soft Cl, Br or I ligands and hemidirected (lone pair is stereochemically active) for relatively harder donor ligands (O, N) that are connected to one another (e.g. in chelates, bidentates or ring systems). Molecular orbital calculations show more charge transfer from ligands (Cl, Br, and I) to the 6p orbitals on lead. This added charge does not increase the p-character of the lone pair orbitals, but increase the p-character of the Pb^{II}–X bonding orbitals so that the NBO lone pair orbital on Pb(II) remains predominantly s-character. For relatively harder donor ligands (O, N) hemidirected structures were calculated to have more net +ve charge on Pb(II) ion than holodirected structures and hence are energetically favored.

8. Conclusions and outlook

The significant development of thia and selena macrocycles called attention to the potential of the tellurium analogues resulting in many publications devoted to macrocyclic polytelluroethers appearing in the literature. However, their total count is still very small compared to that of selena and thia-macrocycles. The considerable and continuing interest in them is due to (1) the enhanced ligating properties of these ligands to transition metal ions and (2) the availability of ^{125}Te NMR spectroscopy to monitor the structures in solution. A novel contribution to the chemistry of tellura macrocycles has been made by reporting a variety of tellurium containing macrocycles *via* more facile and reproducible synthetic routes. Significant developments have been noticed in the field of telluraporphyrins. A peculiar alteration of the reactivity of the telluophene unit within a core modified telluraporphyrin is observed. ^{125}Te NMR is used for structural characterization of the ligands and the complexes in solution. The high reactivity of the Te–C bond is demonstrated by the easy heterolytic cleavage towards metal centres like Hg(II) and Pt(II). Although many new macrocycles involving Te donors and their metal complexes are now known, the development of tellurium containing macrocycles and their metal ion complexes is still in its infancy and there does seem enormous scope for further growth. These macrocycles can be used for complexation with heavy metals due to (1) higher stability constant of

the complexes over their open chain analogs due to macrocyclic effect and (2) selectivity of the metal ion binding can be achieved by varying macrocyclic ring sizes and donor atom set combinations. Also, telluracrown ethers should bind strongly to precious metals like, copper, silver, gold, palladium and platinum since these metals generally prefer soft donor atoms. Considering the weakness of C–Te bond compared to C–S and C–Se bonds and toxicity of organotellurium compounds, the synthesis of tellurium macrocycles and their further chemistry will likely challenge and engage chemists for years to come.

Acknowledgements

I express my sincere gratitude to the Department of Science and Technology (DST), New Delhi, India for financial support under Fast Track for Young Scientist Scheme and to the Birla Institute of Technology & Sciences, Pilani-Goa Campus for support. I also thank Prof. A.B.P. Lever and one of the referees for their constructive comments and Dr. R.N. Behera, Dr. I. Gupta, Dr. R. Panda and Ashish for their helpful suggestions and support. The American Chemical Society, The Royal Chemical Society, Elsevier and Wiley InterScience are gratefully acknowledged for permission to reproduce the figures.

References

[1] E.G. Hope, W. Levason, Coord. Chem. Rev. 122 (1993) 109.
[2] V.P. Litvinov, V.D. Dyachenko, Russ. Chem. Rev. 66 (1997) 923.
[3] W. Levason, S.D. Orchard, G. Reid, Coord. Chem. Rev. 225 (2002) 159.
[4] W. Levason, G. Reid, Comprehensive Coord. Rev. II 35 (2004) 399.
[5] W. Levason, G. Reid, J. Chem. Soc., Dalton Trans. (2001) 2953.
[6] A. Panda, Coord. Chem. Rev. 253 (2009) 1056.
[7] (a) W. Levason, S.D. Orchard, G. Reid, Organometallics 18 (1999) 1275;
(b) A.J. Barton, W. Levason, G. Reid, J. Organomet. Chem. 579 (1999) 235;
(c) W. Levason, S.D. Orchard, G. Reid, J.M. Street, J. Chem. Soc., Dalton Trans. (2000) 2537.
[8] A.K. Singh, S. Sharma, Coord. Chem. Rev. 209 (2000) 49.
[9] W. Levason, G. Reid, in: F. Davillanova (Ed.), Handbook of Chalcogen Chemistry, RSC, 2006, p. 81 (Chapter 2.2).
[10] A. Ulman, J. Manassen, F. Frolow, D. Rabinovich, Tetrahedron Lett. (1978) 1885.
[11] A. Ulman, J. Manassen, F. Frolow, D. Rabinovich, J. Am. Chem. Soc. 101 (1979) 7055.
[12] L. Latos-Grażyński, E. Pacholska, P.J. Chmielewski, M. Olmstead, A.L. Balch, Angew. Chem. Int. Ed. Engl. 34 (1995) 2252.
[13] E. Pacholska, L. Latos-Grażyński, Z. Ciunik, Chem. Eur. J. 8 (2002) 5403.
[14] (a) M.R. Detty, S.L. Gibson, J. Am. Chem. Soc. 112 (1990) 4086;
(b) M.R. Detty, S.L. Gibson, Organometallics 11 (1992) 2147;
(c) M.R. Detty, A.E. Friedman, A. Oseroff, J. Org. Chem. 59 (1994) 8245;
(d) M.R. Detty, F. Zhou, A.E. Friedman, J. Am. Chem. Soc. 118 (1996) 313;
(e) D.E. Higgs, M.I. Nelen, M.R. Detty, Org. Lett. 3 (2001) 349;
(f) C. Francavilla, M.D. Drake, F.V. Bright, M.R. Detty, J. Am. Chem. Soc. 123 (2001) 57.
[15] M. Abe, D.G. Hilmey, C.E. Stilts, D.K. Sukumaran, M.R. Detty, Organometallics 21 (2002) 2986.
[16] M. Abe, Y. You, M.R. Detty, Organometallics 21 (2002) 4546.
[17] M. Abe, M.R. Detty, O.O. Gerlits, D.K. Sukumaran, Organometallics 23 (2004) 4513.
[18] E. Pacholska, L. Latos-Grażyński, Z. Ciunik, Angew. Chem. Int. Ed. 40 (2001) 4466.
[19] E. Lukevics, P. Arsenyan, S. Belyakov, O. Pudova, Chem. Heterocycl. Compd. 38 (2002) 763.
[20] (a) R.J. Gillespie, Can. J. Chem. 39 (1961) 318;
(b) R.J. Gillespie, J. Chem. Edu. 47 (1970) 18.
[21] P.J. Chmielewski, L. Latos-Grażyński, M.M. Olmstead, A.L. Balch, Chem. Eur. J. 3 (1997) 268.
[22] A. Ulman, J. Manassen, J. Am. Chem. Soc. 97 (1975) 6540.
[23] A. Ulman, J. Manassen, F. Frolow, D. Rabinovich, Tetrahedron Lett. (1978) 167.
[24] H. Fujihara, T. Ninoi, R. Akaishi, T. Erata, N. Furukawa, Tetrahedron Lett. 32 (1991) 4537.
[25] Y. Takaguchi, E. Horn, N. Furukawa, Organometallics 15 (1996) 5112.
[26] N. AL-Salim, T.A. Hamor, W.R. McWhinnie, J. Chem. Soc., Chem. Commun. (1986) 453.
[27] W.F. Liaw, C.H. Lai, S.J. Chiou, Y.C. Horng, C.C. Chou, M.C. Liaw, G.H. Lee, S.M. Peng, Inorg. Chem. 34 (1995) 3755.
[28] S. Bali, A.K. Singh, P. Sharma, J.E. Drake, M.B. Hursthouse, M.E. Light, Inorg. Chem. Commun. 6 (2003) 1378.
[29] S. Bali, A.K. Singh, J.E. Drake, M.E. Light, Polyhedron 25 (2006) 1033.
[30] S.C. Menon, H.B. Singh, R.P. Patel, S.K. Kulshreshtha, J. Chem. Soc., Dalton Trans. (1996) 1203.
[31] S.C. Menon, A. Panda, H.B. Singh, R.P. Patel, S.K. Kulshreshtha, W.L. Darby, R.J. Butcher, J. Organomet. Chem. 689 (2004) 1452.
[32] S.C. Menon, A. Panda, H.B. Singh, R.J. Butcher, Chem. Commun. (2000) 143.
[33] U. Patel, H.B. Singh, R.J. Butcher, Eur. J. Inorg. Chem. (2006) 5089.
[34] R. Kaur, S.C. Menon, H.B. Singh, Proc. Indian Acad. Sci. (Chem. Sci.) 108 (1996) 159.
[35] S. Patai, Z. Rapport (Eds.), The Chemistry of Organic Selenium and Tellurium Compounds, vols. 1 and 2, John Wiley and Sons, New York, 1986, 1987.
[36] A. Panda, S.C. Menon, H.B. Singh, C.P. Morley, R. Bachman, T.M. Cocker, R.J. Butcher, Eur. J. Inorg. Chem. (2005) 1114.
[37] S. Panda, H.B. Singh, R.J. Butcher, Chem. Commun. (2004) 322.
[38] S. Panda, S.S. Zade, H.B. Singh, R.J. Butcher, Eur. J. Inorg. Chem. (2006) 172.
[39] S.K. Tripathi, B.L. Khandelwal, S.K. Gupta, Phosphorus Sulfur Silicon 177 (2002) 2285.
[40] S. Srivastava, A. Kalam, J. Ind. Chem. Soc. 83 (2006) 563.
[41] D.W. Johnson, H.K. Mayer, J.P. Minard, J. Banaticla, C. Miller, Inorg. Chim. Acta 144 (1988) 167.
[42] V.W.W. Yam, Y.L. Pui, W.P. Li, K.K.W. Lo, K.K. Cheung, J. Chem. Soc., Dalton Trans. (1998) 3615.
[43] K. Kobayashi, H. Izawa, K. Yamaguchi, E. Horn, N. Furukawa, Chem. Commun. (2001) 1428.
[44] K. Kobayashi, N. Deguchi, O. Takahashi, K. Tanaka, E. Horn, O. Kikuchi, N. Furukawa, Angew. Chem. Int. Ed. 38 (1999) 1638.
[45] H. Citeau, K. Kirschbaum, O. Conrad, D.M. Giolando, Chem. Commun. (2001) 2006.
[46] M.J. Hesford, W. Levason, M.L. Matthews, G. Reid, Dalton Trans. (2003) 2852.
[47] V. Chandrasekhar, R. Thirumoorthi, Organometallics 26 (2007) 5415.
[48] M.B. Robin, P. Day, Adv. Inorg. Chem. Radiochem. 10 (1967) 247.
[49] (a) X. Xu, W. Li, X. Lu, X. Lui, Xuaxue Xuebao 51 (1993) 1170;
(b) H. Xu, W. Li, X. Lui, L. Shen, X. Mao, M. Li, Huaxue Xuebao 52 (1994) 386, Chem. Abstr. 1994, 121, 25539n.
[50] X. Liu, W. Li, X. Lu, H. Xu, Chin. Chem. Lett. 3 (1992) 589.
[51] S. Katsunari, S. Toshio, H. Kazunori, K. Nobumsa, Nippon Kagakkai Koen Yokoshu 85 (2005) 995.
[52] H. Koji, M. Emi, S. Toshio, H. Kazunori, K. Nobumasa, Nippon Kagakkai Koen Yokoshu 86 (2006) 1163.
[53] T.N. Srivastava, A.K.S. Chauhan, G.K. Mehrotra, Synth. React. Inorg. Met. -Org. Chem. 12 (1982) 705.
[54] D.S. Grubisha, G.A. Mirafzal, L.K. Woo, Inorg. Chim. Acta 361 (2008) 3079.
[55] W. Levason, S.D. Orchard, G. Reid, Chem. Commun. (2001) 427.
[56] M.J. Hesford, W. Levason, M.L. Matthews, S.D. Orchard, G. Reid, Dalton Trans. (2003) 2434.
[57] A.J. Barton, A.R.J. Genge, N.J. Hill, W. Levason, S.D. Orchard, B. Patel, G. Reid, A.J. Ward, Heteroatm. Chem. 13 (2002) 550.
[58] S.C. Rawle, G.A. Admans, S.R. Cooper, J. Chem. Soc., Dalton Trans. (1988) 93.
[59] A. Panda, S.C. Menon, H.B. Singh, R.J. Butcher, J. Organomet. Chem. 623 (2001) 87.
[60] R.J. Gillespie, Chem. Soc. Rev. 21 (1992) 59.
[61] C.W. Perkins, J.C. Martin, A.J. Arduengo, W. Lau, A. Alegria, J.K. Kochi, J. Am. Chem. Soc. 102 (1980) 7753.
[62] R.F. Ziolo, J.M. Troup, J. Am. Chem. Soc. 105 (1983) 229.
[63] T.S. Cameron, R.B. Amero, R.E. Cordes, Cryst. Struct. Commun. 9 (1980) 533.
[64] L. Livny, J.P. Glusker, C.W. Bock, Inorg. Chem. 37 (1998) 1853.